國 立 交 通 大 學

奈 米 科 技 研 究 所

碩 士 論 文

探討微米尺寸的基底結構對於細胞貼附型態與生長的影響

Effects of Micron-Scale Patterned Substrates on Cell Morphology, Growth and Cell Cycle Progression

研 究 生 ： 馮玟菲 **Wen-Fei Fong**

指導教授 ： 柯富祥 教授 **Prof. Fu-Hsiang Ko**

中 華 民 國 九 十 八 年 六 月

探討微米尺寸的基底結構對於細胞貼附型態與生長的影響

Effects of Micron-Scale Patterned Substrates on Cell Morphology, Growth and Cell Cycle Progression

研 究 生：馮玟菲　　Student：Wen-Fei Fong

指導教授：柯富祥 教授　　Advisor：Prof. Fu-Hsiang Ko

國 立 交 通 大 學

奈 米 科 技 研 究 所

碩 士 論 文

A Thesis
Submitted to Institute of Nanotechnology
College of Engineering
National Chiao Tung University
in partial Fulfillment of the Requirements
for the Degree of
Master
in

Nanotechnology

June 2009
Hsinchu, Taiwan, Republic of China

中華民國九十八年六月

探討微米尺寸的基底結構對於細胞貼附型態與生長的影響

學生：馮玟菲　　指導教授：柯富祥 教授

國立交通大學奈米科技研究所碩士班

摘 要

為了瞭解並調控細胞與移植材料介面間的作用行為，我們製造了一維的密集線與二維的密集柱狀陣列，兩種不同地貌的表面，試圖去了解材料的表面圖案是如何影響細胞貼附後的種種行為。利用微影技術，不僅可以容易的定義出欲探討的表面圖案，更可以精準的製作成我們想要研究的的地貌尺寸。在實驗中，以微影曝光並加以蝕刻製作成之矽基材，做為母模，利用翻模的方式，製作了具有 1 微米大小的線寬與柱狀直徑表面的 PDMS 基材，其圖案深度皆為 350 奈米，希望藉此探討微米尺度下的地貌表面，對於子宮頸癌細胞貼附及生長的調控。

在我們的實驗結果發現在一維密集線表面生長貼附的細胞，傾向與溝槽平行且對齊排列生長，與二維的密集柱狀陣列表面與平滑的材料表面相比較，生長於平行溝槽的細胞整合蛋白(integrin-α5)的表現增加，且細胞有更為良好貼附的現象。此外，在細胞的型態上，貼附於二維的密集柱狀陣列表面與平滑的材料表面細胞，多呈現圓球態表面多絲狀偽足伸出，貼附狀況差，伴隨著腫瘤抑制蛋白(p53)的表現，基質金屬蛋白酶 9(MMP-9)的表達增高。

由結果我們得知，藉由外在地貌的差異，進而影響由細胞表面整合蛋白(integrin)所介導的訊號傳遞，造成了細胞生長、DNA 合成、細胞移動以及凋亡的不同結果產生。如此，藉由改變細胞貼附的基底材質地貌，進而改變細胞中由

整合蛋白所介導的訊號傳遞而影響細胞行為，將會是生醫材料及生醫工程上很好的應用及操作細胞的方式。

Effects of Micron-Scale Patterned Substrates on Cell Morphology, Growth and Cell Cycle Progression

Student: Wen-Fei Fong Advisor: Prof. Fu-Hsiang Ko

Institute of Nanotechnology

National Chiao Tung University

Hsinchu 300, Taiwan, ROC

Abstract

In order to find the ways for controlling the cell-material interface, we made two different topographies of one dimensional (1D) periodic lines/space pattern and two dimensional (2D) arrayed pillars pattern for cell behavior analysis. Here we used lithographic techniques can control not only the topographic pattern but also the scale of such topography within microscale ridge widths (~1μm) and submicron deep grooves (~350nm). We investigated the microscal topography regulated cell functions using human epithelial carcinoma (HeLa) cell culture on poly(dimethylsiloxane) (PDMS), the silicon substrate with microstructures on it were used as templates for micromolding a silicon elastomer, PDMS, into tissue scaffolds for cell patterning purpose. We observed that on 1D periodic lines surface cells tend to align with the direction of microscale ridges and grooves and have better attachment through an

integrin α5 subunit expression compared with 2D periodic pillars pattern or flat PDMS surfaces. By contrast, cells cultured on the 2D periodic pillars and smooth PDMS substrates were mostly round and worse adherent with higher filopodia protruded, tumor suppressor protein 53 (p53) increased and matrix metalloproteinase-9 (MMP-9) expression. Considering the important role of integrin-mediated intracellular signaling in anchorage-dependent cell function, we found the external topography regulate cell function as cell growth, DNA synthesis, motility, and apoptosis. Modulation of cellular morphology related integrin-mediated signaling by altering substrate topography will have useful applications in biomaterials science and tissue engineering.

Acknowledgment

回想碩士班兩年，學到的東西很多，想當然要感謝的人也很多！首先感謝我的指導老師，張雯惠老師以及林俊宏老師，不僅指導我學術及實驗上的知識，更培養了我面對研究該有的態度，非常感謝你們對我的關心及照顧並適時的給予我協助，讓我不被困難擊倒，在學術研究上總能保持不滅的熱情。此外，感謝柯富祥教授，給了我們一個良好的實驗環境以及資源，讓我們充分的發揮，朝著自己有興趣的題目去研究，此外在學術以及態度上的教誨，讓我在專業領域以及待人處事上能更進一步。

感謝在一開始帶領我熟析 NDL 環境的游世明學長，感謝你的細心指導，讓我在短時間內學會了實驗上要用到的機台，也讓我認識了 NDL 的學長群們，讓我在往後遇到實驗上的困難時，總能在最快時間內找到人協助。

感謝 NDL 的學長們，餅叡、大餅、大頭、羊咩、叮噹以及郭珊珊學姊，不僅感謝你們教我機台，也因為有你們在，讓 NDL 倍感溫馨與歡樂；另外感謝我的同學們，諺辰以及叮噹的學弟，在你們在百忙中還給予我機台上的指導。

感謝應化所的廖春雄學長，教我合成的步驟以及原理，還順便合成出現成的分我用，也把你分析的 data 直接給我一份，雖然最後沒能試出好的實驗結果，不過對你的感謝我一直都有放在心上！

感謝柯博實驗室已畢業學長姐們過去的照顧，也感謝還留著的中樞、佳典銘清學長，一直以來對實驗室的貢獻如同實驗的支柱。感謝實驗室的好伙伴們，有鄭捷陪我吃喝玩樂，幫我改英文文法，就像是英文小老師一樣厲害!!實驗室有你在就有一種安全感，每當遇到困難總是會第一時間想到找你幫忙！感謝李伯、林驚蟑、Gigi，有你們在的實驗室很溫馨也很有趣；感謝學弟妹們，你們都很認真也很乖，柯博實驗室有你們真好。

也感謝遠在南投的鍋吃冰、還有台南的舒慧姐，給予我精神上的支持。另外感謝以前在中山醫的學妹碗婷，在實驗上對我的協助頗多，真的是很貼心的學妹，也是很好的小幫手，恭喜你成為我在交大的學妹，希望你在交大能很快的進入狀況，做妳有興趣的研究。

最後，也最重要，感謝我的家人在我的求學路程中總是全力的支持，感謝老哥總是記得要繳學費的事，對家人的感謝，現在的我我無法用言語形容，但在將來我會用行動來說明。

Contents

摘 要 i

Abstract iii

Acknowledgment v

Contents vi

List of Tables vii

List of Figures vii

Chapter 1: Introduction 1
- 1.1 General Introduction 1
- 1.2 Biomaterial 1
  - 1.2.1 Classes and Development 2
- 1.3 Tissue Engineering 5
- 1.4 Mediation of Biomaterial–Cell Interactions 7

Chapter 2: Literature Review 10
- 2.1 The fabrication Strategies Employed to Create Microscale Topography Surface 10
- 2.2 Topological Control of Cell Behavior 12
- 2.3 Substrates With Micro- and Nanofabricated Surfaces Affect Integrin-Mediated Signaling 19
  - 2.3.1 Introduction of Integrin-Mediated Cancer Cell proliferation and Invasion 24
- 2.4 Motivation 25
- 2.5 Organization of the Thesis 26

Chapter 3: Materials and Methods 27
- 3.1 Preparation of Patterned Masters for PDMS Membrane 27
- 3.2 Preparation of PDMS Membrane 28
- 3.3 Cell Culture 29
- 3.4 Cell Growth on Micropatterned Substrates 29
- 3.5 Cell Cycle Analysis by Flowcytometry 30
- 3.6 BrdU Incorporation 30
- 3.7 Western-Blot Analysis 31
  - 3.7.1 Extraction of Whole-cell Protein 31
  - 3.7.2 Determination of Protein Concentration 31

3.7.3 SDS-PAGE and Immunoblotting 31
3.8 Gelatin Zymography 32
3.9 Statistical Analysis 33
Chapter 4: Results and Discussions 34
4.1. Fabrication and Characterization of Systematic effects of patterned elastic PDMS substrate on cell adhesion. 34
4.2. Cells adhere to flat PDMS and 2D periodic pillars patterned PDMS substrate show a retarded G1/S transition. 39
4.3. Protein expressed by integrin-mediated intracellular signal transduction. 42
4.4. Investigation of cell morphology using scanning electron microscopy. 46
Chapter 5: Conclusions 48
Reference 49

List of Tables

Table 1.1 4
Select biomaterials with their classification and examples of their medical application.

Table 2.1 10
Various fabrication techniques used for creating artificial substrates with topography.

Table 2.2 13
Interactions between substrate topography and cells.

List of Figures

Figure 1.1 3
Classification of Biomaterials.

Figure 1.2 6
Tissue engineering strategies are classified into three categories.

Figure 1.3 7
Regeneration of skin tissues using stem cells.

Figure 1.4. ..... **9**
Schematic diagram of microfabrication and nanofabrication of material surface.

Figure 2.1 ..... **17**
SEM images of cells cultured with 4 μm pitch pattern. (A) Cell aligned along the groove direction. (B) At the cell edges, lamellipodia were perpendicular to the patterns and able to adhere to the floor of the grooves.

Figure 2.2. ..... **18**
Spreading had an effect on cell growth and apoptosis. (A) Schematic diagram show the initial patterns containing different size of square. (B) Apoptotic and DNA synthesis index after 24 hours culturing.

Figure 2.3 . ..... **20**
By complex reciprocal molecular interactions between cells and their surroundings, the behavior of the dynamic state of multicellular tissues and individual cells is regulated. Ellipsis (…) indicates that the lists of signals are not complete. PLC, phospholipase C; GAGs, glycosaminoglycans; PGs, proteoglycans; CAMs, cell adhesion molecules.

Figure 2.4. ..... **22**
Organization of focal adhesions. Focal adhesions are streak-like elongated structures and anchor the bundles of actin stress fibers (F-actin) which located at the periphery through αvβ3 integrins and clustering structural proteins like vinculin and talin. Double immunolabeling for αv (red) and α5 (green) as cells attaching to fibronectin, exhibited the separation between fibrillar and focal adhesion. ECM: extracellular matrix.

Figure 3.1 ..... **28**
The fabrication procedure of patterned Si substrate by utilizing the semiconductor process.

Figure 4.1 ..... **35**
Effects of different patterned substrates on cell morphology and growth. (A) Cell cultured on a smooth silicon oxide substrate which serves as an internal control surface. (B-F) represented the cells grew on 1D periodic line/space pattern. (G-K) showed the cells grew on 2D periodic pillars pattern. The dimension of pattern is 500

nm, 1 μm, 5 μm, 10 μm and 20 μm, respectively.

Figure 4.2 ..... **37**

SEM images of flat PDMS surface (A), 1D periodic line/space (1μm width) PDMS surface (B) and 2D periodic pillar (1μm diameter) PDMS surface (C). Optical microscope images of HeLa cells cultured for 24h on bacteriological grade polystyrene Petri dish (D), flat PDMS surface (E), 1D periodic line/space patterned PDMS surface (F), and 2D periodic pillar patterned PDMS surface (G). (H) The average number of adherent HeLa cells on different patterned PDMS surface. Statistical significance assessed by one-way ANOVA tests is shown as *:$p<0.05$ when compared with polystyrene Petri dish control and #: $p<0.05$ when compared with flat PDMS control.

Figure 4.3 ..... **40**

Analysis of cell cycle phases. The cell cycle of HeLa cells cultured on smooth and patterned PDMS substrates for 24h. Cellular DNA was stained with propidium iodide and analyzed by flow cytometry. (A) The DNA content of cells of the cell cycle. (B-C) A histogram represents the percentage of total cells in G1 phase, S phase and G2/M phase, respectively. Statistical significance assessed by one-way ANOVA tests is shown as *:$p<0.05$ when compared with polystyrene Petri dish control and #: $p<0.05$ when compared with flat PDMS control.

Figure 4.4 ..... **41**

BrdU incorporation in HeLa cells cultured on Petri dish, smooth and patterned PDMS substrates. Exponentially growing HeLa cells were incubated with BrdU and the incorporation rate was analysed by immunofluorescence. Statistical analysis was done using ANOVA. The star marks the statistically significant difference in BrdU incorporation at $p<0.05$ when compared with polystyrene Petri dish control and # marks the statistically significant difference at $p<0.05$ when compared with flat PDMS control.

Figure 4.5 ..... **42**

(A) Immunoblotting of transmembrane integrin proteins (α5); focal adhesion-associated adaptor protein, paxillin; tumor suppressor protein, p53 (B) Activity of matrix metalloproteinase 9 (MMP-9) analyzed by gelatin zymography.

Figure 4.6 ..... **46**

Morphology of human epithelial carcinoma HeLa cells cultured on Petri dish (A),

smooth bare silicon (native oxide) surface (B), 1D periodic line silicon (native oxide) surface, and 2D periodic pillar silicon (native oxide) surface for 24hr imaged by scanning electron microscopy. Areas of lower cell density were selected to facilitate observation of individual cell shapes. The images of the cells shown in the selected micrographs are typical of cells throughout the culture.

Chapter 1: Introduction

1.1 Poly (dimethyl siloxane) microstructure replication

Photolithography, a process which uses light to engraves the exposure pattern into the material underneath the photo resist, can also be used for microfabrication of tissue engineering structures. However, traditional photo-lithography suffers from diffraction problems and more expensive and new lithographic processes are therefore required. E-beam writing has been proved recently to be a powerful tool for fabricating micro/nanostructures and replicated by using imprinting, embossing and other contact replication technologies. Soft lithography has been developed in the 1990s [1], opened up opportunities for culturing or probing cells with biomimetic surfaces that can be engineered with chemical and topographical features. Currently the popular silicone elastomer poly-dimethyl siloxane (PDMS), which is cheap and widely used for making biological materials or microfluidic devices due to its desirable properties such as easy replica molding, good optical transparency, biological compatibility and ease of bonding to seal patterned structures [2]. So, here we used a poly-dimethylsiloxane (PDMS) casting techniques for patterning 1D and 2D microstructure surface with different feature sizes. And for its good transparent properties, it would be useful for directly observing the responses of cells to external conditions.

1.2 Introduction of Biomaterial

The study of biomaterials has existed for around half a century not a new area of science, encompasses elements of medicine, biology, chemistry, tissue engineering and materials science. It is a provocative field with steady and strong growth over its history, and many companies investing large amounts of money into the development

of new products.

The term, biomaterials, has many definitions and difficult to formulate, one common definition of biomaterials as: “A biomaterial is any material, natural or man-made, that comprises whole or part of a living structure or biomedical device which performs, augments, or replaces a natural function”. Moreover, another definition of biomaterial such as "any substance (other than drugs) or combination of substances synthetic or natural in origin, which can be used for any period of time, as a whole or as a part of a system which treats, augments, or replaces any tissue, organ, or function of the body". In 1986, biomaterials were first defined in the Consensus Conference of the European Society for Biomaterials as a nonviable material used in a medical device, intended to interact with biological systems.

1.2.1 Classes and Development

Not only as a powerful set of clinical tools for patient treatment, biomaterials also found in virtually every instrument, device, implant, or piece of equipment in the operating room. For the ongoing development of biomaterials, surgeons have driven clinical application of biomaterials and stand uniquely positioned historically. Moreover, in the properties of a particular material, depend not only on the chemical nature of its atoms, but also on their arrangement and distribution in its microstructure (grains, pores, etc). Due to the staggering variety of these materials and their possible combinations, materials with specific thermal, mechanical, nuclear, electrical, magnetic and optical properties can be fabricated but there is still a huge amount of research that needs to be done.

In the classification of biomaterials, there exist 4 classes that include metals, ceramics, natural and synthetic polymers **(Fig. 1.1)**.

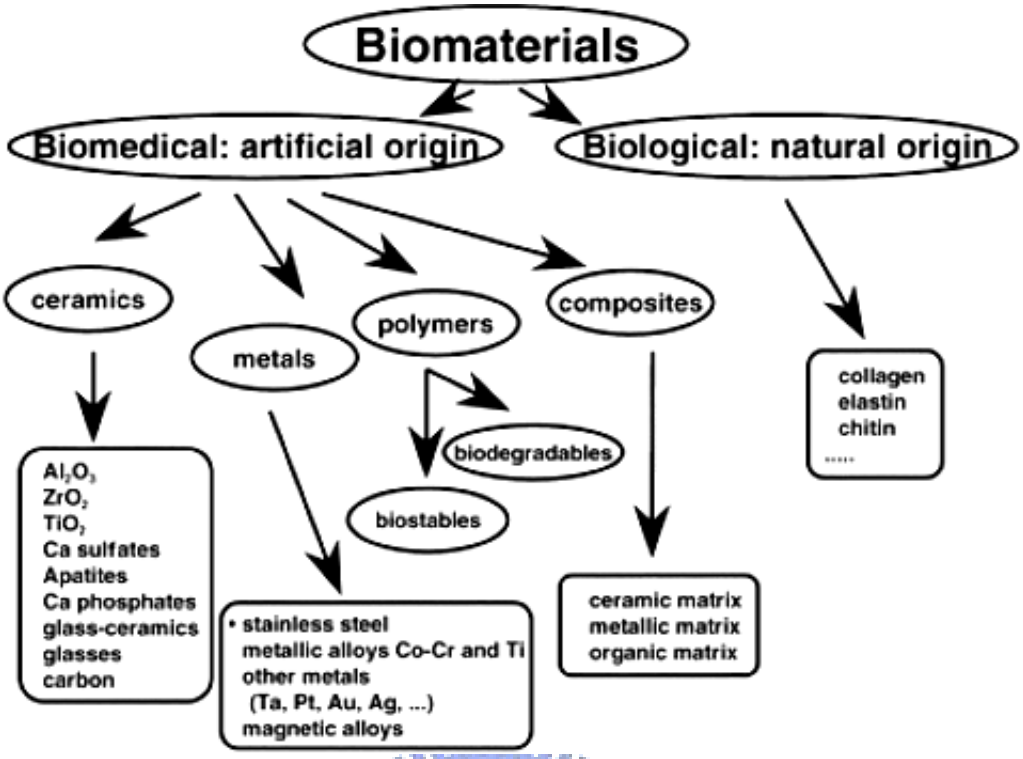

Figure 1.1 Classification of Biomaterials [3]

Biomaterials are widely used in medical to improve or restore diseased tissues or organs, but their effectiveness is questionable. During the process of materials selection, the general situation in which the material is to be used and how the characteristics of available materials will reflect its performance should take into account. Toxicity must be avoided but inertness is not a high priority in biomaterials. The examples of biomaterials and their applications see **Table 1.1**. Alloys and hydroxyapatites were introduced in orthopaedic and dental fields and satisfactory results were obtained. However, metallic and ceramic biomaterials are not suitable to replace soft tissues unfortunately, because of its markedly different mechanical properties. So far, polymers are used as the most disposable medical devices, but new functional biomaterials are awaited.

Table 1.1	Select biomaterials with their classification and examples of their medical applications [4].	
Classification	Biomaterial	Examples of applications
Metal	316L stainless steel	Surgical instruments, orthopedic fixation devices, stents
Metal	Titanium and titanium-containing alloys	Fracture fixation, pacemaker encapsulation, joint replacement
Metal (shape memory alloy)	Nickel–Titanium Alloy (Nitinol)	Stents, orthodontic wires
Metal	Platinum and platinum-containing alloys	Electrodes
Metal	Silver	Anti-bacterial material
Polymer	Polytetrafluoroethylene (PTFE, Teflon®, Gore-Tex®)	Vascular grafts, catheters, introducers
Polymer	Poly(ethylene terephthalate) (polyester, Ethibond, Dacron®)	Vascular graft, drug delivery, non-resorbable sutures
Polymer	Poly(methyl methacrylate) (PMMA)	Bone cement, intraocular lens
Polymer	Polyurethane	Catheters, tubing, wound dressing, heart valves, artificial hearts
Polymer	Silicone rubber (polydimethylsiloxane PDMS)	Catheters, feeding tubes, drainage tubes, introducer tips, flexible sheaths, gas exchange membranes
Polymer	Polycarbonate	Major component in renal dialysis cartridge, heart-lung machine, trocars, tubing interconnectors
Polymer	Hydrogels (poly(ethylene oxide), poly(ethylene glycol), poly(vinyl alcohol), etc.)	Drug delivery, wound healing, hemostasis, adhesion prevention, contact lenses, extracellular matricies, reconstruction
Polymer	Polyamides (nylon)	Non-resorbable sutures
Polymer	Polypropylene (ie, prolene)	Non-resorbable sutures, hernia mesh
Ceramic	Alumina	Joint replacement, dental implants,

		orthopedic prostheses
Ceramic	Carbon	Heart valves, biocompatible coatings, electrodes
Ceramic	Hydroxyapatite	Implant coatings, bone filler
Ceramic	Bioglass	Metal prostheses coating, dental composites, bone cement fillers

As this thesis is concerned with the development and testing of poly (dimethlysiloxane) (PDMS)-based cell substrate, a detail description about the advantages of the polymeric biomaterials used in this study as its biocompatibility and ease of processing will be described follows.

1.3 Tissue Engineering

In cellular engineering and regenerative medicine, a significant amount biomaterial science research has been focused and the discipline from the application of synthetic materials for treatment of patients is shifting to the use of synthetic materials for the production of biological products for the treatment of patients. Therefore, as central in the design of milieus, biomaterials will direct cell behavior and function [5].

Tissue engineering includes engineering to develop tissues that restore, maintain, or enhance tissue function and the use of biological sciences as an interdisciplinary field [6]. Besides, it has particular advantages that can provide a permanent solution to the problem of organ failure over other therapies such as drugs. In general, there are three main strategies [7]: (i) using cell substitutes or isolated cells as cellular replacements, (ii) using acellular biomaterials which can induce tissue regeneration, and (iii) using a cell-seeded materials (in the form of scaffolds) **(Fig. 1.3)**. Despite significant advances that success engineering of organs such as skin and cartilage [8], in making off the-shelf tissue-engineered organs, there are still a lot of challenges remained that includes the lack of a renewable source which cells functioned and immunologically

compatible, a desired material with mechanical, chemical, and biological properties; and a suitable structure that can easily integrate into the complicated architectural native tissues of host's circulatory system with large, vascularized tissues generated.

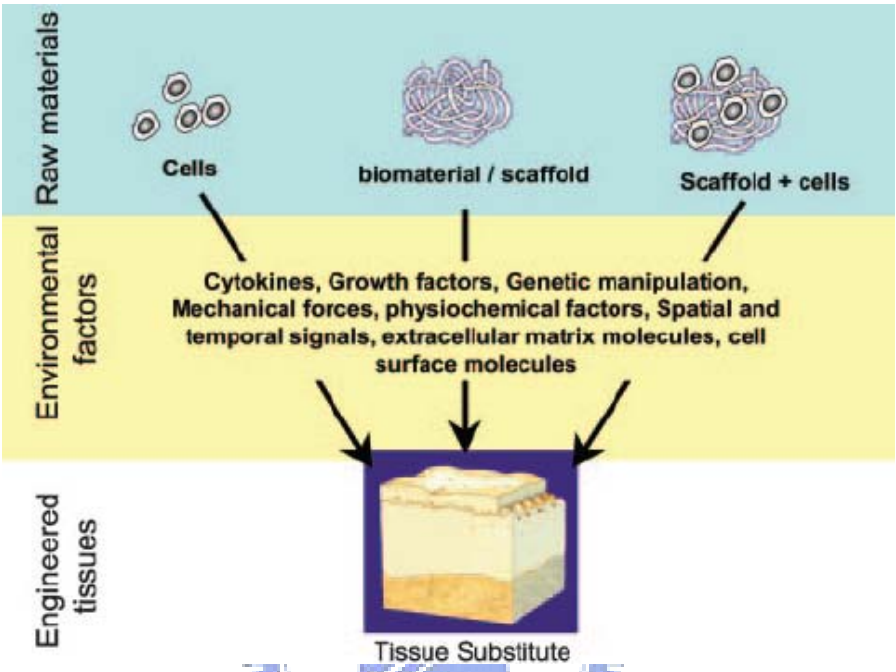

Figure 1.2 Tissue engineering strategies are classified into three categories [7].

The extracellular matrix (ECM) is a natural structural found in tissues for cells supporting and three-dimensional organization. Several strategies utilized the ECM mimicking to manufacture scaffolds for cell migration and proliferation and thus for various types of tissues engineering, including vascular, bladder, and cartilage [9].

Moreover, by using stem cells, tissues now can be engineered comprise a diverse range from thin epithelial layers (cornea, skin and mucosal membranes) to bulk skeletal tissues [10]. These systems are innately different in their physical structure and rate of self-renewal (the two important considerations of any attempt to reconstruct tissues by using stem cells). Selection of the suitable diversities of organ systems with cognate stem cells is essential for developing adequate strategies of specific areas. For example of clinical skin grafting, autografts are produced by

culturing patient's own epidermal stem cells and then transplanting this stem cells along with a suitable dermis-like substrate to generate an epidermal sheet [11] **(Fig. 1.3)**.

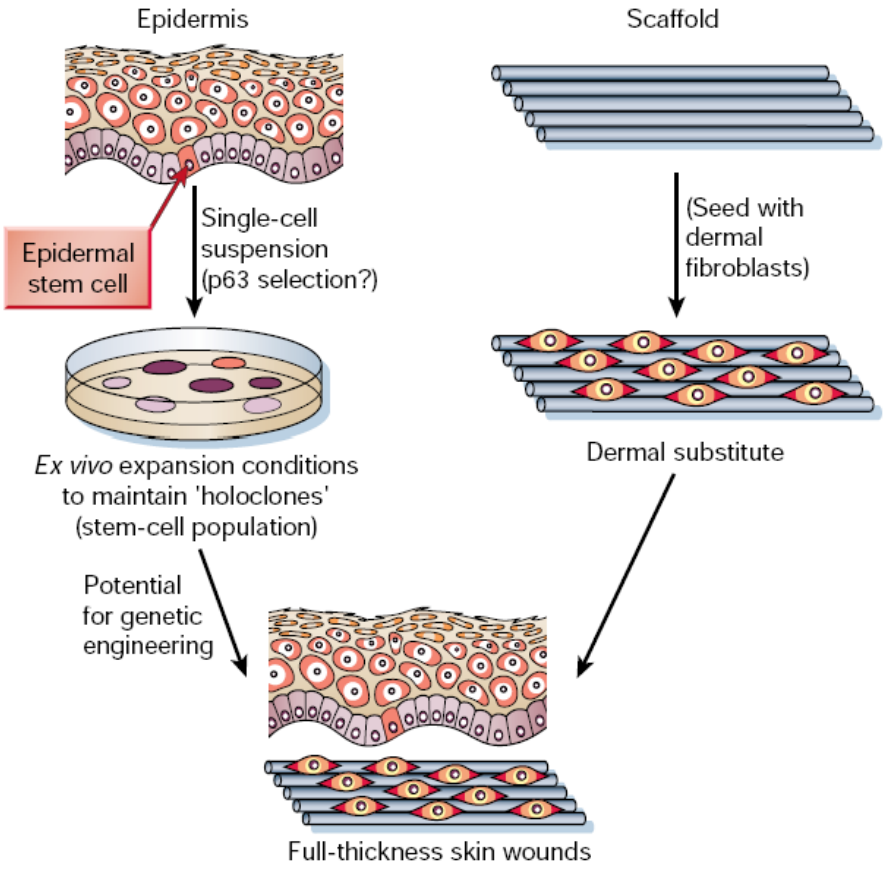

Figure 1.3 Regeneration of skin tissues using stem cells [10].

1.4 Mediation of Biomaterial–Cell Interactions

As defined, the science of biological surface is a broad interdisciplinary area where biological environments and processes at interfaces between synthetic materials are investigated and bio-functional surfaces are fabricated.

An appropriate implanted surface with proper cellular response is essential for tissue regeneration and integration. Coupling of protein layers to the surface may provide a way for surface functionalization to transform a bio-inert material into a

biomimetic or even bio-active material. There are different requirements to functionalize biomaterials, taking for examples: biosensors and biochips for diagnostics, bioelectronics, medical implants in the human body, tissue engineering [12], biomimetic materials and artificial photosynthesis.

In most examples above, biorecognition is a central determination. Any approaches to make a functional, sophisticated surface for bio-material interactions must take into account on the molecular scale for the ability of biological systems to recognize the specially designed features. Famous examples are enzyme–substrate, antibody–antigen, and transmitter-receptor (in cell membranes) recognition. And through their 3D topographic architecture combination, the recognition is programmed into the superimposed chemical properties, the molecules and the dynamic architecture. Therefore, for designing a desirable surface with specific biological function must take these conditions into account.

Interestingly, when cells are present, there is a remarkable unique synergistic connection between the nanometer and the micrometer length scales although the fundamental interactions occur on the molecular scale theoretically [13].

In order to match the specific bio-recognition ability of biological systems, biofunctional surfaces need advanced design and preparation. This requires in particularly combined with chemical, topographic and visco-elastic patterns on surfaces to match the nanometer-scale proteins and micrometer-scale cells.

Intrinsically all methods of bio-surface science are useful. Since the instrument for measuring miniaturized surface has been developed, like high-resolution microscopies (e.g. scanning probe), spatial problems are resolved, moreover, non-invasive optical spectroscopies, high sensitivity, nano- and microfabrication and self-organizing monolayers are important for bio-surface science. In addition, nanofabrication and microfabrication of material surfaces offer the opportunity to

develop functional scaffold and enhance cell attachment **(Fig. 1.4)**. A suitable artificial scaffold supports cells proliferation and interaction with neighboring cells with a tissue specific microenvironment. Its surface properties effect cell adhesion, migration, viability, and even direct cell differentiation.

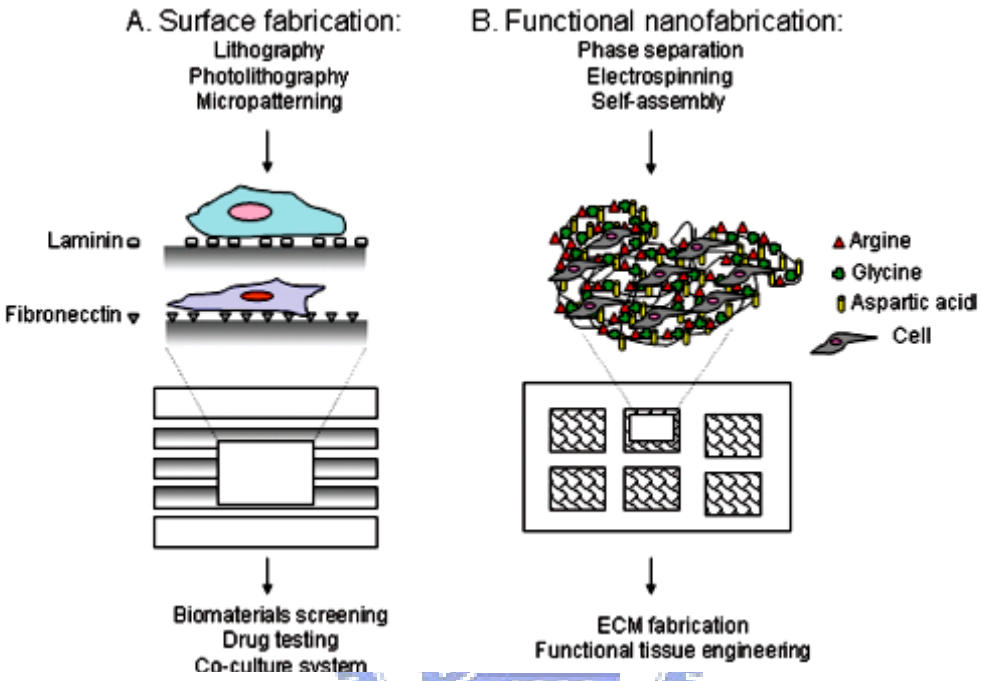

Figure 1.4 Schematic diagram of microfabrication and nanofabrication of material surface [14].

Chapter 2: Literature Review

2.1 The Fabrication Strategies Employed to Create Microscale Topography Surface

A list of several fabrication strategies employed to create synthetic substrates with topography is given in **Table 2.1**. Micro-fabrication technique is a potentially powerful tool for solving some of the challenges in tissue engineering [15]. Such as Micro-Electro-Mechanical Systems (MEMS), an integration of electronics, mechanical elements actuators, and sensors on a silicon substrate through microfabrication technology can be used to control features at length scales from <1 μm to >1 cm [1] and employed for biomaterial fabrication. The majority of the studies used photolithography to produce with dimension-controlled features and specific forms.

Table 2.1 Various fabrication techniques used for creating artificial substrates with topography [16]

Fabrication technique	Material	Feature frequency
Photolithography and reactive ion etching, UV and glow discharge treatment	PDMS cast of silicon original	Equal groove and ridge width [17]
Photolithography and reactive ion etching	Quartz	Equal groove and ridge width [18]
Photolithography and anisotropic etching, glow discharge	Titanium coated silicon	Equal groove and ridge width [19]
Cutting with diamond or tungsten	Polystyrene, epoxy replicas	5-30 μm repeat spacing [20]
Electron-beam lithography and wet etching, glow discharge treatment	PDMS cast of silicon original	Grooves separated by 4 μm-wide ridges [21]
Solution polymerization	PDMS gels of varying	3, 4, 15 μm periodicity

	softness	[22]
Microporous filter: Nylon dip-coated with PVC/PAN copolymer	Uncoated and silicon coated filters	0.2–10 μm diameter, spacing not listed [23]
Particle settling	Poly(NIPAM) particles on polystyrene surface	2D hexagonal lattice, 0.96μm avg. distance between sphere centers [24]
Fiber-optic light conduit-fused quartz cylindrical fibers placed on agarose-covered coverslips	Fused quartz	12-13 or 25 μm radii, spacing not listed [25]
Acid washing, electropolishing, sandblasting, plasmasprayed Ti	Titanium	Random [26]
Alumina emulsion polishing, grinding with SiC paper	Ti, Ti/Al/V alloy, TiTa alloy	Random [27]
Scratching with glass rod	Polystyrene and H_2SO_4-treated polystyrene	Random [28]
Coating glass with protein and withdrawing liquid to orient protein	Oriented collagen or fibrin	Size and spacing of fibers not listed [29]
ECM replication-PMMA polymerization casting followed by polyurethane solution casting	Polyurethane positive cast of PMMA negative	Micron and nanometer scale topography, similar to ECM [30]

Other techniques employed to manufacture surface features with controllable dimensions include GLAD (glancing angle deposition, a patented thin-film deposition process) [31], laser ablation (the process of removing material from a solid) [32] and deposition (PLD, pulsed laser deposition) [33], replica molding of X-ray lithography masters (lithography method using X-ray to expose the resist; due to shorter wavelength of X-ray radiation (0.4 - 4 nm) thus allows higher resolution) [34], imprint lithography (a contact process, can be made with high-resolution but low-throughput) [35], and ink-jet printing (also known as micro-drop technique) [36].

Some techniques are capable of fabricating nanometer scale features. However electron-beam lithography, is the most developed, high-resolution lithographic technique known, and has been used to fabricate features as small as 50 nm over large areas.

These techniques are now being integrated into biomaterials to facilitate cell–material composites fabrication which can be employed for tissue engineering. Alternative methods to fabricate scaffolds with micro- and nano-scale features include tissue spin casting, electro-spinning of nanofibers, 3D printing, and microsyringe deposition. In 3D printing method, polymer particles and salt are mixed and printed by using a bonding agent, and once the salt dissolved, the composition forms a porous scaffold [37].

Although a comprehensive technology which has been used to fabricate various scaffolds is beyond the scope of this report, they are coming out as powerful methods of fabricating tissue engineering scaffolds. In addition, microscale technologies allow a powerful ability to control the microenvironment for cell adhesion and miniaturize assays for high-throughput applications.

2.2 Topological Control of Cell Behavior

Independent of biochemistry, topographical cues from the extracellular matrix may have significant effects on cellular behavior. Studies have demonstrated that substratum topography has direct effects on the ability of cells orientation, migration, and organization of cytoskeleton. Basement membranes are thin sheets which composed of extracellular matrix (ECM) proteins and spread through the vertebrate body, serving as substrates for constructing cellular structures. The topography of basement membranes is a composite meshwork by pores, fibers, and ridges in features of nanometer sized dimensions. Synthetic surfaces fabricated with micro-

and nanoscaled topographical features have been shown to influence cell behavior. These accounts lead to the hypothesis that in regulating cellular behavior, the topography of the basement membrane may plays an important role independent from that of the chemistry of the basement membrane.

In addition to chemical and physical-mechanical properties, basement membranes possess a complex, three-dimensional topography which consist of micro- and nanometer sized features. Physical topography is known to affect cell behavior. Paul Weiss, among others, pioneered the field of "contact guidance" during the 1930s, 1940s and 1950s [38]. As early as 1962 and 1963, Rosenberg claimed that nanometer sized features influence cellular behavior [39]. Despite recognition of the importance of substratum topography, relatively little is known about the effects of topographical features of nanometer scale on cell behavior.

A lot of reports have indicate that interactions between substrate topography and cells were changed with cell types and substratum features including ridges, fibers, steps, pores, nodes, grooves, wells and adsorbed proteins. **Table 2.2** summarizes the literature, providing a list of feature type, fabrication technique used, substratum material, feature size and spacing, cell type studied, and the cellular effect generated by the surface features.

Table 2.2	Interactions between substrate topography and cells [16]	
Feature type	Cell type studied	Cellular effect
Grooves/ PDMS cast of silicon original 2, 5, 10 μm width 0.5μm depth	Rat dermal fibroblasts	Microfilaments and vinculin aggregates oriented along 2 μm grooves after 1, 3, 5, and 7 days, but was less oriented on 5 and 10 μm grooves; vinculin located primarily on surface ridges; bovine and endogeneous fibronectin and

		vitronectin were oriented along grooves; groove-spanning filaments also observed [40]
Grooves and pits/ Titanium-coated epoxy replicas of silicon original V-shaped grooves 35-165 μm width 30, 60, and 120 lm depth V-shaped pits 35-270 μm width and 30, 60, 120 μm depth	Rat parietal bone implant model	Mineralization occurred often on grooved or pitted surfaces, but rarely on smooth control surfaces; frequency of formation of bonelike foci increased decreased as groove depth increased; frequency of mineralization increased as depth of pit increased; bonelike foci oriented along long axis of grooves [41]
Grooves and chemical pattern / Ti, Au-coated polyurethane treated with fibronectin, alkane thiols V-shaped grooves 25, 50 μm width depth not listed	Bovine capillary endothelial cells	Cells adhered to regions coated with fibronectin, which adsorbed to regions silanized with methyl but not tri(ethylene glycol)-terminated silanes; cells attached to either grooves or ridges, depending on which possessed the methyl-terminated silane and fibronectin coatings [42]
Ridges/ Polystyrene cast of silicon original 0.5-100.0 μm width 0.03-5.0 μm height	*Uromyces appendiculatus* fungus	Maximum cell differentiation observed for ridges or plateaus 0.5 μm high; ridges higher than 1.0 μm or smaller than 0.25 μm were not effective signals; ridge spacing of 0.5-6.7 μm caused high degree of orientation of the fungus [43]
Waves/ PDMS gels of varying softness Softer gels had smaller waves while hard gel had larger waves	Human dermal fibroblasts and keratinocytes	Fibroblasts proliferated equally on all substrates; keratinocytes spread more and secreted more ECM on soft gels than on hard gel [22]

Wells and nodes/ PDMS cast of silicon original Square nodes or wells 2, 5, 10 μm diameter	ATCC human abdomen fibroblasts	Cells on 2 and 5 μm nodes showed increased rate of proliferation and increased cell density compared to cells on 2 and 5 μm wells; 10 μm nodes and wells did not differ statistically from smooth surfaces [44]
Pillars and pores/ PMMA, PET, polystyrene Circular pillars and pores 1, 5, 10, 50 μm diameter	Human osteoblasts and amniotic epithelial cells	Cells engulfed pillars or stretched between adjacent 1 and 5 μm pillars; cells attached to edges of pores, especially on 10 μm pores; texture caused increase in cell adhesion on all materials but PMMA; greatest increase in adhesion was on 50 μm PET pillars [45]
Pores/ Uncoated and silicon coated filters 0.2–10 μm diameter depth not listed	In vivo canine model	Non-adherent, contracting capsules around implants with pores smaller than 0.5 μm; implants with 1.4-1.9 μm pores showed adherent capsules but no inflammatory cells; pores bigger than 3.3 μm were infiltrated with inflammatory tissue; pores 1-2 μm allowed for fibroblast attachment [23]
Spheres/ Poly(NIPAM) particles on polystyrene surface 0.86-0.63 μm diameter when temperature raised from 25 to 37 ℃	Neutrophil-like induced HL-60 cells	Cells loosely adhered but did not spread on spherecoated surface and could roll easily; excess active oxygen released when temperature was increased on spherecoated surface, but not on poly(NIPAM) grafted surface[24]
General roughness/ Ti, Ti/Al/V alloy, TiTa alloy 0.04, 0.36, and 1.36 μm peak-to-valley heights	Human gingival fibroblasts	Cells aligned to grinding marks: 10% of cells oriented on surface with 0.04 μm roughness, 60% on 0.36 μm roughness, and 72% on 1.36 μm roughness [27]
Protein tracks/ Glass coated with fibronectin	BHK cells, rat tendon fibroblasts, rat dorsal root ganglia cells,	Fibers increased spreading and alignment in direction of fiber; actin aligned in fibroblasts; alignment of

0.2–5 μm width	P388D1 macrophages	focal contacts in fibroblasts and macrophages; increased polymerization of F-actin; fibers increased speed and persistence of cell movement and rate of neurite outgrowth; macrophages had actin-rich microspikes and became polarized and migratory [46]
Microtextured surface/ Polyurethane positive cast of PMMA negative Micron and nanometer scale topography	Bovine aortic endothelial cells	Cells grown on replicas of ECM spread faster and spread areas at confluence which appeared more like cells in their native arteries than cells grown on untextured control surfaces [30]

Grooves are the most common feature type employed in studies for the influence of surface structure on cells. In general, investigations of grooved surfaces revealed that most cells aligned **(Fig. 2.1)** accompany with organization of actin and cytoskeleton elements paralleling to the grooves.

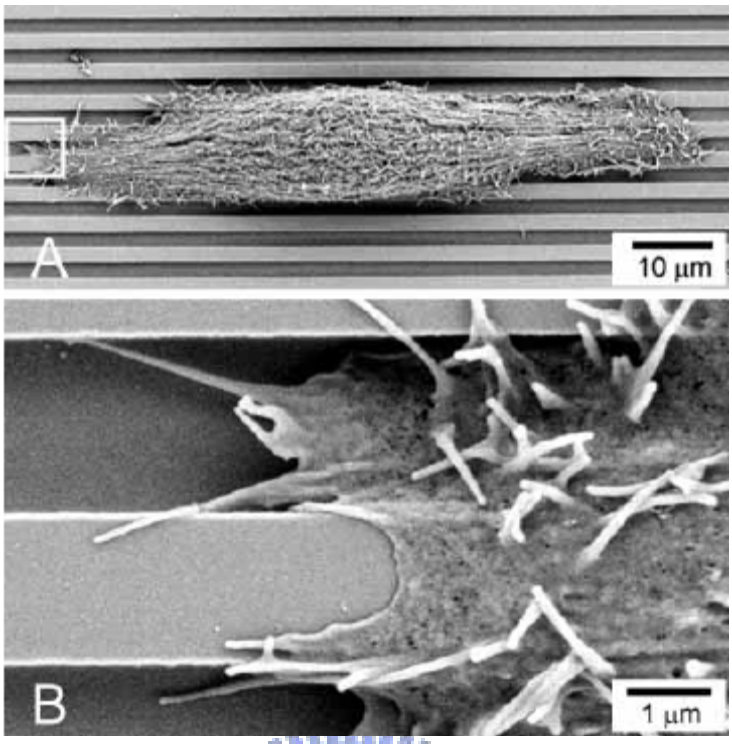

Figure 2.1 SEM images of cells cultured with 4 μm pitch pattern. (A) Cell aligned along the groove direction. (B) At the cell edges, lamellipodia were perpendicular to the patterns and able to adhere to the floor of the grooves [47].

Oakley and Brunette found that microtubules were the first element to align to grooves, followed by actin assembly, 20 minutes after cell plating [48]. In order to maximize their contact area, oblong focal adhesions (1-10 μm long) [49] orientated along the direction of the ridges, leading to an alignment of cytoskeleton elements and of the cell body as a whole. Many studies found that the depth of grooves was more important than their width in determining cell orientation [50]. Orientation often increased with increasing depth, but decreased with increasing groove width. In other words, as ridge width or groove width increased, the orientation phenomena of cells on grooves diminished.

In the literature, there are some studies investigating the behavior of cells on other synthetic features, including wells and pores, nodes, and spheres. Green and coworkers found that, compared to 10 μm nodes and smooth surfaces, nodes of 2 and

5 μm resulted in increased cell proliferation [44]. Fujimoto et al. investigated the behavior of cells on spheres and observed that cells responded to a change in sphere size which produced by an increasing in temperature [24]. The cells released excess active oxygen when sphere diameters shrunk as a result of the temperature being increased from 25 to 37℃. Chen et al. thought cell spreading also varied while changing the spacing between multiple islands by maintaining the total cell-matrix contact area constant [51]. No matter what the type of integrin antibody or matrix protein is used to mediate adhesion, cell shape was found to determine whether individual cells grow or die **(Fig. 2.2)**.

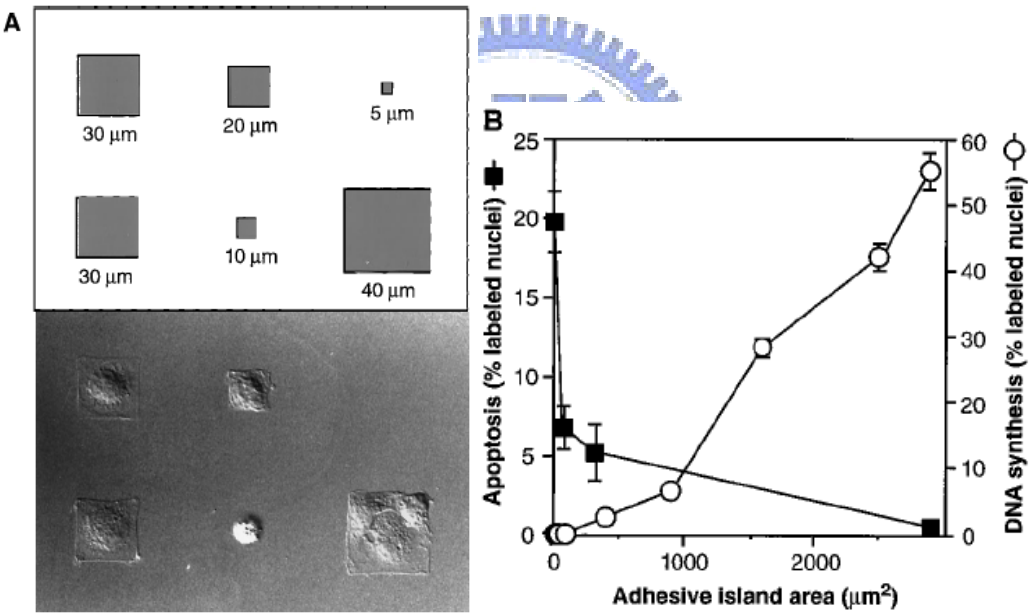

Figure 2.2 Spreading had an effect on cell growth and apoptosis. (A) Schematic diagram show the initial patterns containing different size of square. (B) Apoptotic and DNA synthesis index after 24 hours culturing [51].

The fact that basement membranes are incorporated into cell adhesion and extension processes which composed of unique and intricate topographies. It can be seen that coupled with topographical features have been shown to influence cell behavior, leads to the hypothesis that the topography of the basement membrane

plays an important role in regulating cellular behavior distinct from the chemistry of the basement membrane.

2.3 Substrates With Micro- and Nanofabricated Surfaces Affect Integrin-Mediated Signaling

Tissue dynamics is the regeneration, function and formation after damage (as function in pathology), it result an complex spatial and temporal coordination of cell fate processes, which is induced by a numerous signals generating from the extracellular microenvironment [52] **(Fig. 2.3)**.

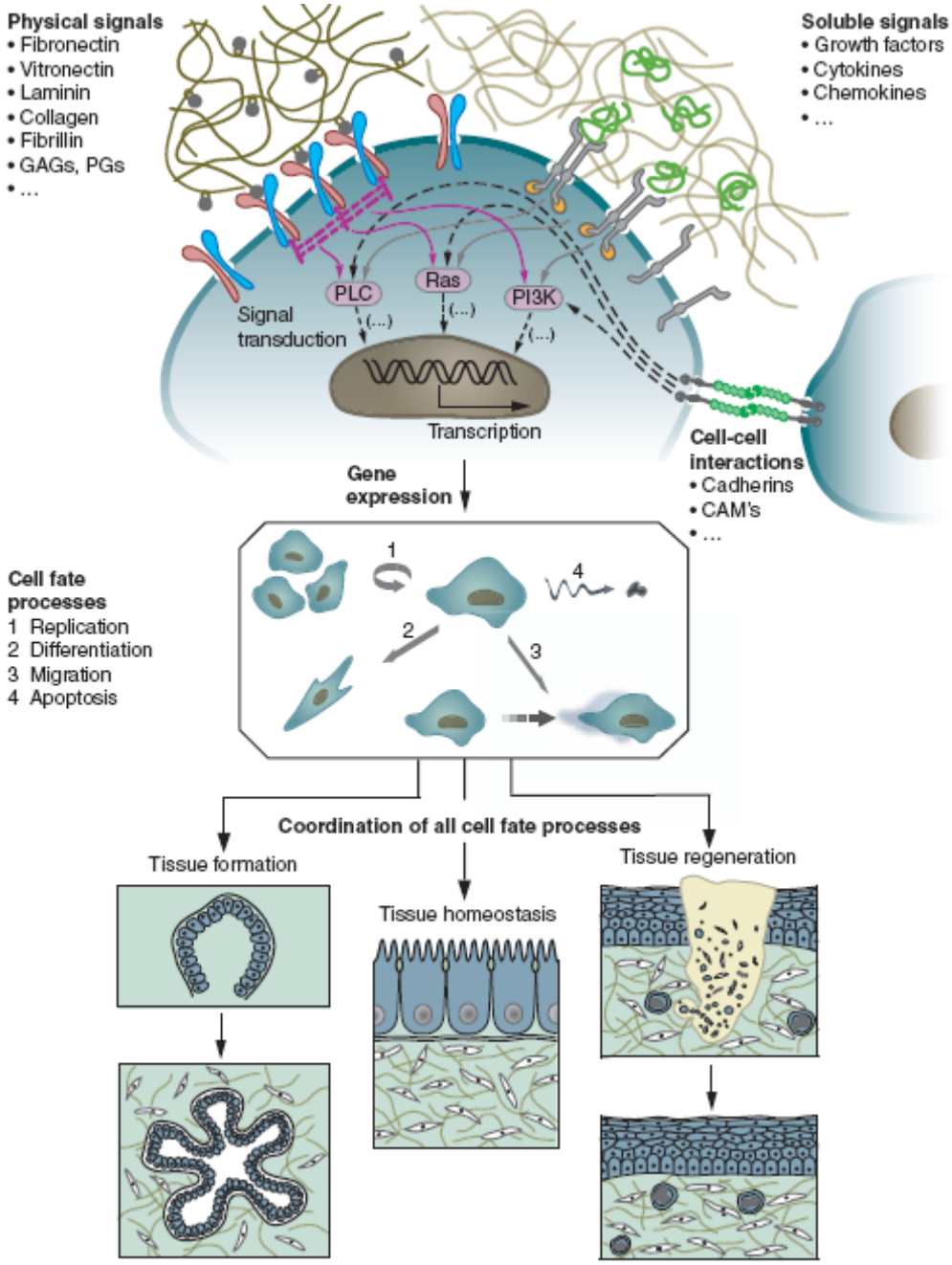

Figure 2.3 By complex reciprocal molecular interactions between cells and their surroundings, the behavior of the dynamic state of multicellular tissues and individual cells is regulated. Ellipsis (…) indicates that the lists of signals are not complete. PLC, phospholipase C; GAGs, glycosaminoglycans; PGs, proteoglycans; CAMs, cell adhesion molecules [5].

A concise summary of interactions between cells and their surroundings , intricate and highly biochemical dynamic and biophysical signals, transmitted from cell membrane by various surface transmembrane receptors and integrated by intracellular

signaling cascade, convert to regulate gene expression and alter cell phenotype ultimately.

In migrating cells, these receptors act as the “anchor” plates to support adhesion to the ECM or via adapters with actin filaments inside the cell to link other cells. As described above, the integrins act as receptors to mediate cell attachment and migration.

The integrins are a superfamily of cell adhesion receptors consisting of α– and β–chains with short cytoplasmic and large ligand-binding extracellular domains **(Fig. 2.4)**. As the integrins bind to ligands of the extracellular portion, it leads to the changing of interactions between α– and β–chain cytoplasmic domains and integrin clustering by conformational changing in the receptors [53]. Although integrins do not have any catalytic activity, signal transduction is through the direct and indirect interactions with many coupled integrins.

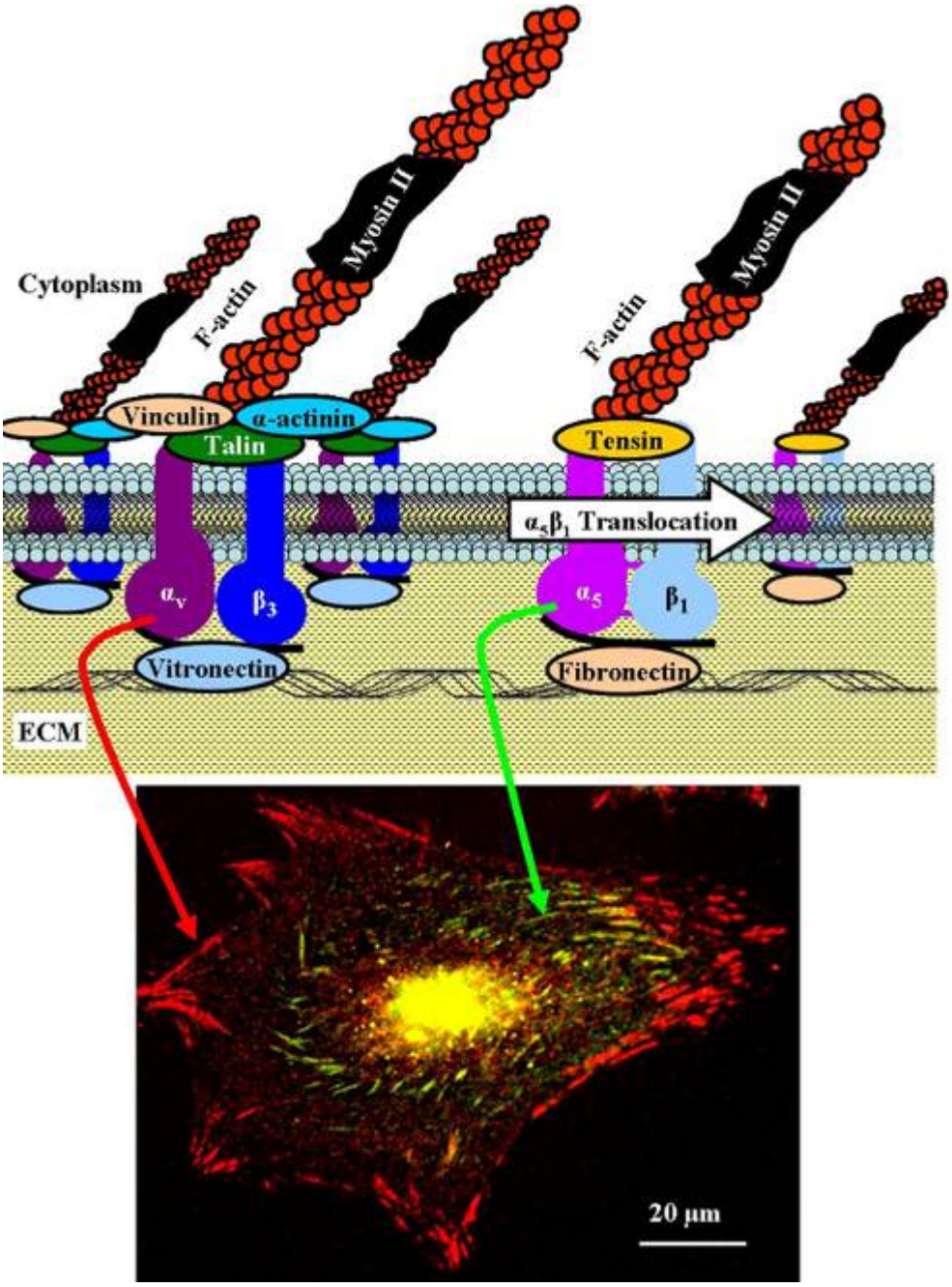

Figure 2.4 Organization of focal adhesions. Focal adhesions are streak-like elongated structures and anchor the bundles of actin stress fibers (F-actin) which located at the periphery through αvβ3 integrins and clustering structural proteins like vinculin and talin. Double immunolabeling for αv (red) and α5 (green) as cells attaching to fibronectin, exhibited the separation between fibrillar and focal adhesion. ECM: extracellular matrix [54].

The fundamental of physiology is the cells responsive interactions on surfaces, and that will induce pathological condition or tumor if deregulated. Just like physiological

tissues, adhesion of cells to substrates in plastic culture dishes is primarily mediated by integrins binding to ECM proteins. In cell cycle regulation, these interactions between cell surface and extracellular matrix play a critical role, leading to proliferation or death [55], and they also regulate receptor-mediated responses to other signals. Thus, for the strategy of migration-related disorders, a thorough understanding of the cell adhesion mechanisms will facilitate development of therapies.

On the development of surface patterning techniques with μCP, it is possible to examine the importance of the spatial dimensions systematically over the occurrence chemical interactions. In the late 1990s, a pioneering study on SAM-coated ECM proteins islands surfaces with endothelial cells [51], and on a hydrophilic background nonspecific bindings were resisted. Thus, by the binding of ECM through transmembrane protein integrins, cell spreading was controlled, and by this way, the size and shape of cells were controlled by the patterned features. While keeping the direct contact area constant, researchers could also restricted the attainability of cell spreading by adjusting the pattern spaces and feature sizes between them. They found that the footprints of cells play an outstanding role in switching cell proliferation, growth, apoptosis and regulating cycle, correlated with the cell spreading and imposed cell shape. In addition, cytoskeletal anchorage to the focal adhesion complexes via integrins contacting to the external environment substrate, related studies also pointed to the importance of the cytoskeleton (e.g. actin) in mediating the cellular responses [56].

In the last several years, a lot of studies have taken advantage of surfaces patterned techniques to study the interactions between spatial controlled surface and the specificity of cell morphology and adhesion, migration, dendritic branching and mechanical transduction (how mechanical signals convert into the intracellular

chemical responses) by using microfabricated surface which made of elastomeric PDMS.

2.3.1 Introduction of Integrin-Mediated Cancer Cell Proliferation and Invasion

Cell survival depends on multiple elements, including extrinsic physical signals, the soluble extracellular matrix (ECM) survival/growth factors and the signals from cell–cell interactions. Normal cells undergo apoptosis (a physiological form of programmed cell death) when stressful conditions occur such as DNA damage, or when these signals are interrupted. Apoptosis contributes the most tissues and organs program to the normal morphogenesis, failing to regulate apoptosis are closely correlated with abnormalities development and the pathophysiology of cancer and autoimmune diseases [57].

Signals from the ECM are important in turning to mature tissues and maintaining normal cytoarchitecture, because for cell growth and survival, most normal cell types exhibit anchorage-dependence. However, during metastatic process, cells display altered adhesive and migratory properties, lose the anchorage dependence, and allowing them to metastasize to appropriate environments for surviving and growing. Therefore, it is important to understand how the ECM signals suppress cell death at the molecular level, and when the signals are lost what pathway of apoptotic is initiated in normal cells.

Apoptosis can be triggered by multiple progressions. There is strong evidence that as the instable genomic were generated the tumor suppressor protein p53 response to conditions by mediating apoptosis [58]. Moreover, cells also undergo apoptosis when lacking of survival signals from soluble factors and/or ECM survival signals which transduced by the receptors and/or integrins [59].

It has not been established whether there is a role for p53 in encouraging an

apoptotic pathway when ECM survival signals are absent. However, in many malignant cell types mutations in p53 are common. The fact that for growth and survival, these cells are no longer anchorage dependent, it is consistent with the hypothesis that survival signals from ECM which transmited by integrins, suppress p53-regulated apoptosis.

In addition, MMPs can affect many growth factors, such as chemokines, cytokines, cell surface adhesion receptors and cell migration, all of them relate with tumor growth and metastasis [60].

Matrix metalloproteinases (MMPs; matrixins) are a family of structurally related enzymes, and according to structural features they are currently grouped. The majority of MMPs are secreted into the extracellular matrix (ECM), thus far, >20 MMPs have been identified in mammals and all are produced as inactive zymogens and are activated by proteolysis,

2.4 Motivation

Adhesion of live cells to external surfaces plays an important role in many cellular processes such as cell growth, differentiation, motility, and apoptosis. Cell adhesion involves the interaction of cells with other cells or with the extracellular matrix (ECM) and is of great importance in the development of disease in multi-cellular organisms. Much of the current knowledge regarding biological processes has been obtained through in-vitro studies in bulk aqueous solutions or in conventional Petri dishes, with neither methodology accurately duplicating the actual in-vivo biological processes. Although this strategy has led to important findings, it is not an exact representation of the in vivo situation. Recently, a number of innovative approaches have attempted to address these shortcomings by providing substrates with controlled features. In particular, tunable surface chemistries and topographical micro and

nanostructures have been used as model systems to study the complex biological processes. To understand in more detail how cell behavior, we exposed cells to geometrically patterned substrata, which were created using computer software and transferred to a silicon wafer (master) by lithographic techniques.

2.5 Organization of the Thesis

In order to finding the ways for controlling the bio-implant interface, in this thesis we made two different topographies of one dimensional (1D) periodic lines/space pattern and two dimensional (2D) arrayed pillars pattern for cell behavior analysis. Here we used lithographic techniques can control not only the topographic pattern but also the scale of such topography within microscale ridge widths (~1μm) and submicron deep grooves (~350nm). We investigated the microscal topography regulated cell functions using human epithelial carcinoma (HeLa) cell culture on poly(dimethylsiloxane) (PDMS). The silicon substrate with microstructures on it were used as templates for micromolding a silicon elastomer, PDMS, into tissue scaffolds for surface patterning purpose.

In Chapter 1, the general overview of the classification and development of biomaterials was introduced. There is an overview of the history of tissue engineering and the mediation between biomaterial and cell interactions. Literature reviews describe various fabrication strategies which employed to create synthetic substrates with microscale topography and discuss how topological can control cell behavior by microscale topography surface in Chapter 2. The details of fabrication processes, protein expression analysis and characterization of detection and analysis instruments are presented in Chapter 3. In Chapter 4, the modulation of integrin-mediated signaling by altering substrate topography was discussed. Finally, the summary of important achievements and contributions of this thesis are addressed in Chapter 5.

Chapter 3: Materials and Methods

3.1 Preparation of Patterned Master for PDMS Membrane

Fig. 3.1 shows the fabrication procedure of the patterned silicon substrate by utilizing the semiconductor process. The master substrate is the silicon wafer. To have the enough protection in the subsequent etching, the oxide film with the thickness of 550 nm was used as the hard mask and was formed on the silicon substrate with a wet oxidation process at 980°C in the ASM/LB45 furnace. The patterns were defined by the electron-beam lithography. The negative tone resist used here was Sumitomo NEB22 with a thickness of 400 nm. The electron-beam patterning was performed on the Leica WEPRINT200 operated at 40 KeV. After the resist development, the patterns were transferred to the oxide layer by the RIE oxide etcher (TEL TE5000) and then transferred into the silicon substrate by the TCP poly-silicon etcher (LAM Research Co., TCP 9400SE) with a designed depth of 1.2 μm. Finally, the resist was stripped and the oxide layer was removed by dipping the sample into the HF solution.

Comparing with other techniques of microfabricating for investigation of cell adhesion and cell growth, using photolithography as a tool can easily fabricate a variety of micro/nano-scale pattern and manufacture a regular periodic pattern that help us to identify the conformation of ECM which can really affect the cellular behavior.

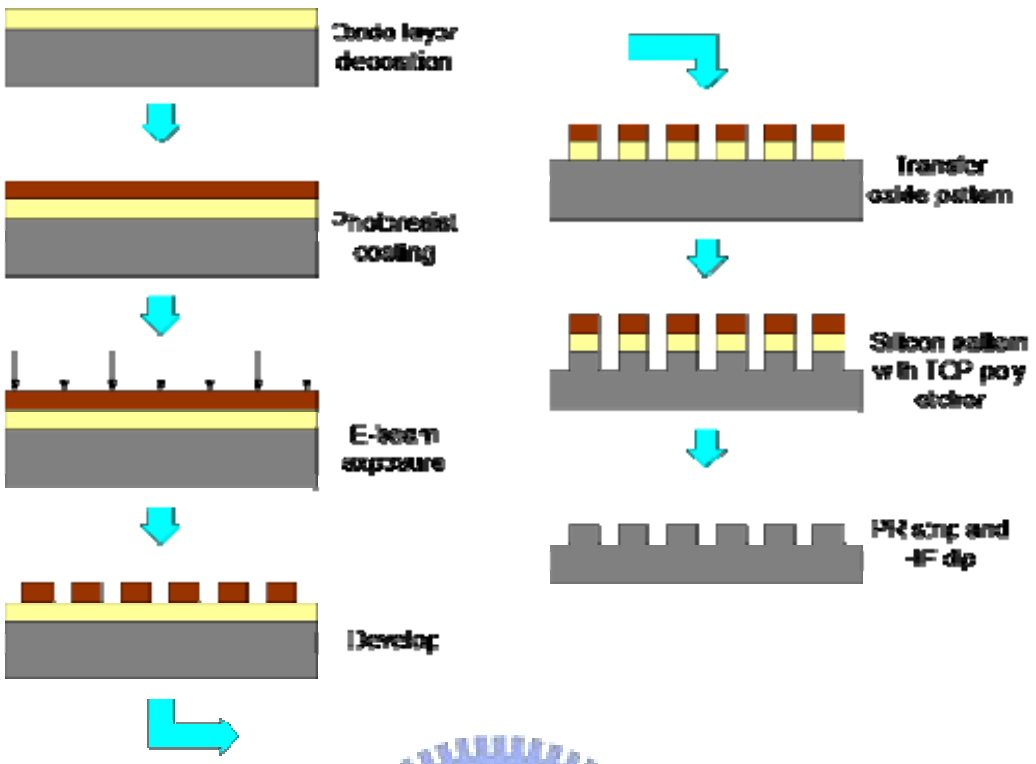

Figure 3.1 The fabrication procedure of the patterned Si substrate by utilizing the semiconductor process.

3.2 Preparation of PDMS Membrane

The patterned silicon substrate was used as the reusable master for making the PDMS membrane. The PDMS mixture was made from a 10:1 ratio of Sylgard 184 Silicone Elastomer base and curing Agent (Dow Corning Corporation, Midland, MI), by weight. The liquid mixture of PDMS was thoroughly mixed and was poured on the master to a resultant thickness of approximately 5 mm. The PDMS coated substrate was then cured at room temperature for 24 hours. Finally, the PDMS membrane was then manually peeled away from the glass wafer with the use of tweezers. Once the PDMS stencils were fabricated, they were sterilized with 70% ethanol, then rinsed thrice with DD water, and stored in sterile bags until needed.

3.3 Cell Culture

The human cervical cancer cell line, HeLa, was obtained from the American Type Culture Collection (Rockville, MD). The cells were grown in 90% DMEM supplemented with 10% FBS, 100 units/mL penicillin G and 100 μg/mL streptomycin. The incubation was carried out at 37°C under humidified atmosphere of 5% CO_2 in air. The pH values of media and buffers used in this study were adjusted to 7.4. Medium was filtered through a 0.22-μm-pore size filter before use. Medium was changed twice weekly. All cells were used between four and seven passages after receipt.

3.4 Cell Growth on Micron-patterned Substrates

HeLa cells were cultured in 100-mm tissue-culture dishes for maintenance. When the cells were 80% confluent, the culture medium was replaced with new medium and then subcultured for experiments. To explore the influence of geometrically patterned substrate on cell behaviors, HeLa cells were seeded to patterned PDMS substrate. The sterile PDMS stamps were put into traditional culture dish, and immerged in culture medium. Cell suspension at density of 5×10^5 cells/ml were added into each dish and further incubated for 24 hours. PDMS stamps, with the characteristic of light transmittable, were used for microscopic observation. In addition, cells were also grown for flowcytometric analysis. After seeding, most cells were attached to the PDMS stamps. There were two types of patterns with the dimension of 500 nm, 1 μm, 5 μm, 10 μm and 20 μm, respectively. The smooth areas between the patterned fields acted as internal controls.

3.5 Cell Cycle Analysis by Flowcytometry

For flow cytometric analysis, a FACSCalibur flow cytometry (Becton Dickinson, NJ) equipped with a single Argon ion laser was used. Forward light scatter (FSC), which is correlated with the size of the cell, and the right-angle light scatter (SSC), which is correlated with the complexity of the cytoplasm, were used to establish size gates and exclude cellular debris from the analysis. At the end of incubation, the silicon wafers were removed to another clear dish. After rinsed twice with PBS, the adherent cells on silicon wafers were trypsinized for detach, washed with PBS, then fixed in PBS-methanol (1:2, volume/volume) solution and, finally, maintained at 4°C for at least 18 h. Following two more washes with PBS, the cell pellet was stained with the fluorescent probe solution containing PBS, 40 μg/ml propidium iodide and 40 μg/ml DNase-free RNaseA for 30 min at room temperature in the dark. DNA fluorescence of PI-stained cells was evaluated by excitation at 488 nm and monitoring through a 630/22-nm band pass filter. A minimum of 10,000 cells were analyzed per sample, and the DNA histograms were gated and analyzed further using Modfit software on a Mac workstation to estimate the percentage of cells in various phases of the cell cycle.

3.6 BrdU Incorporation

At the end of incubation after 48 hr, cells were labeled with 10 μM BrdU for 6 h. After fixation with ice cold 70% ethanol for 1 h, store at -20°C overnight or for several days. Pellet cells were resuspended in 2 mM HCl/0.5% TritonX-100 and incubated for 30 min at room temperature. After centrifugation, cell pellets were resuspended in 0.5 ml of 0.1 M Na2B4O7, pH 8.5, and after a PBS wash, cells were stained with 1ml of antibody solution (1 ml PBS containing 0.5% Tween-20/1% BSA + 10μl FITC-conjugated mouse anti-BrdU monoclonal antibody) for 1 h at room

temperature in the dark, washed, and resuspended in 5 mg/ml of propidium iodide solution. After 30 min, the cells were analyzed by two-dimensional flow cytometry.

3.7 Western-Blot Analysis

3.7.1 Extraction of Whole-cell Protein

After 24 hr of culturing, cells were scrapped from culture dishes or plates with a policeman and collected in 1.5 ml of eppendorfs. Cell pellets were spined down at 3,000 g at 4℃ for 5 min and the supernatants were discarded. Cell pellets were resuspended with proper amount of cell lysis buffer, incubated on ice for 30 min, and disrupted by vortex every 5 min. After that, cell lysate was centrifuged at 14,000 g at 4℃ for 15 min and transferred to a new 1.5 ml of eppendorf. Proteins were stored at -80℃.

3.7.2 Determination of Protein Concentration

The protein concentration was measured by the Bio-Rad protein assay kit. Protein samples were diluted in 1/25 with 1x PBS. For quantification, the standard BSA protein was diluted from 400 μg/ml to 25 μg/ml by a 1:2 serial dilution. 10 μl of each standard diluent or protein sample was pipetted into 96-well ELISA plates in triplicate. 200 μl of dye reagent was added into each sample-containing well and another three empty wells for blank. The absorbance of protein solution was read at 590 nm by ELISA reader.

3.7.3 SDS-PAGE and Immunoblotting

About 30-50 μg of cell lysate was mixed with 3x sample buffer in a 1.5 ml of eppendorfs, denatured by boiling water for 10 min then chilled on ice. Samples were loaded into 10% polyacrylamide gel, stacked at 80 V for 30 min, and then resolved at

100 V for 60-90 min. Separated protein was transferred onto PVDF membranes in protein transfer buffer at 330 mA for 60-90 min. Membrane blocking was done by rinsing the PVDF membranes with TBST containing 5% skim-milk and incubated at 37℃ for 1 hour with shacking. The PVDF membranes were then incubated overnight at 4℃ with primary antibodies in proper dilution. After removal of the primary antibodies, the PVDF membranes were washed with TBST three times with five min each. Hybridization of secondary antibody was done at 37℃ for 1 hour. The membranes were washed with TBST three times with five min each. Immuno-reaction protein bands were visualized in ECL chemiluminescence system.

3.8 Gelatin Zymography

Gelatinase secretion of cell culture supernatants was determined by zymography with gelatin as substrate for MMP-2 and MMP-9. Briefly, serum-free conditioned medium was collected from confluent culture of the cells after 24 hr culturing. 20 μl were mixed with sodium dodecyl sulphate (SDS) sample buffer, and without prior denaturation, were run on an 10% SDS-polyacrylamide gel electrophoresis containing 1 mg/mL of gelatin. After electrophoresis, the gels were washed in 2.5% Triton X-100 for 1 h at room temperature to remove the SDS and incubated for 48 h at 37°C in a renaturing buffer containing 50 mmol/L Tris (pH 7.5), 10 mmol/L $CaCl_2$, 150 mmol/L NaCl, and 0.05% NaN_3 to allow digestion of the gelatin. The gels were subsequently stained in a solution of 0.25% Coomassie brilliant blue G-250 for 30 minutes and destained for 1 h with acetic acid and methanol. Proteolytic activity appeared as clear bands (zones of gelatin degradation) against the blue background of stained gelatin. For quantitation, the bands were scanned and densitometry was performed.

3.9 Statistical Analysis

All numerical values reported represent mean values ± SD. The statistical significance comparing differences between the experimental and control values was evaluated using Student's t test. Asterisks were used to graphically indicate statistical significance ($P < 0.05$) in the figures. All experiments were performed in at least triplicate. Figures were derived from representative experiments.

Chapter 4: Results and Discussions

4.1. Fabrication and characterization of systematic effects of patterned elastic PDMS substrate on cell adhesion.

In order to develop next-generation tissue engineering materials, the understanding of cell responses to novel material surfaces needs to be better understood. Topography presents powerful cues for cells, and it is becoming clear that cells will react to micro-scale surface features, intensely.

Two types of patterned PDMS membranes were fabricated in this study as shown in **Fig. 4.1**. One is one dimensional (1D) periodic lines with equal width and space. The other one is two dimensional (2D) arrayed pillars and dimension of the pillars is half of their period. Fig. 1B-F represented the cells grew on 1D periodic line/space pattern. Cell elongation and alignment on grooves and ridges were observed and in Fig. 1G-K showed the cells grew on 2D periodic pillar pattern. By contrast, when the cells grew on the substrate of 2D periodic pillar pattern, they showed poor adhesion and spreading properties accompanying with growth retardation. The dimension of patterns is 500 nm, 1 μm, 5 μm, 10 μm and 20 μm, respectively. The smooth areas between the patterned fields were acted as internal controls (A). All patterns shown here were on the same PDMS substratum. The cells were grown in the same condition except the difference on substrate patterns.

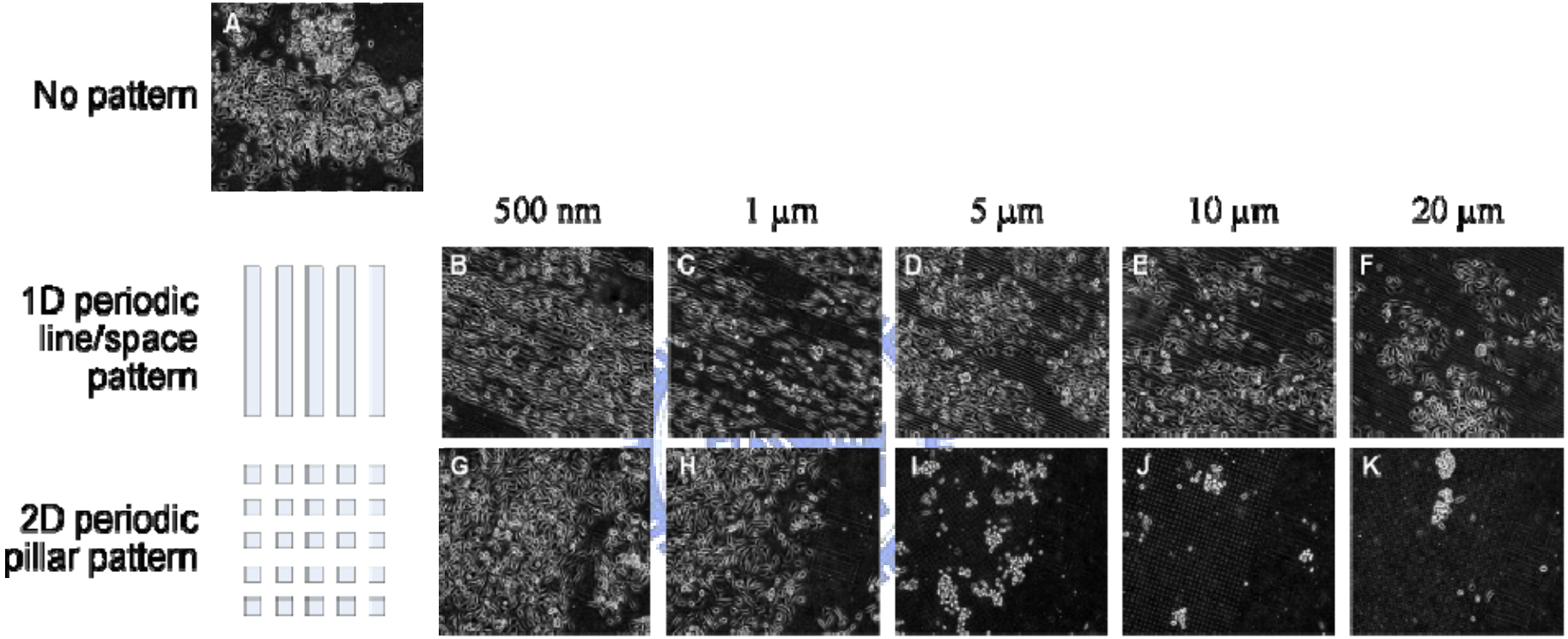

Figure 4.1 Effects of different patterned substrates on cell morphology and growth. (A) Cell cultured on a smooth silicon oxide substrate which serves as an internal control surface. (B-F) represented the cells grew on 1D periodic line/space pattern. (G-K) showed the cells grew on 2D periodic pillars pattern. The dimension of pattern is 500 nm, 1 μm, 5 μm, 10 μm and 20 μm, respectively.

To compare the gradient dimension of patterns, we found that HeLa cells did not spread on 2D periodic pillars when pillar diameter is larger than 5 μm and the adherent cells decreased by increasing pillar dimension (Fig.1I-K). So, here we chose the dimension of 1 μm (1D) periodic lines and (2D) arrayed pillars for our further study because cells adhered on these patterns with conspicuous elongate on 1D periodic lines and opposite circular form on 2D periodic pillars.

This result is consist with the report of Teixeira et al. who demonstrated that [61] with 600 nm deep grooves, the percentage of aligned cells was constant on patterns with pitches ranging from 400 nm to 2000 nm and decreased on 4000 nm pitch patterns.

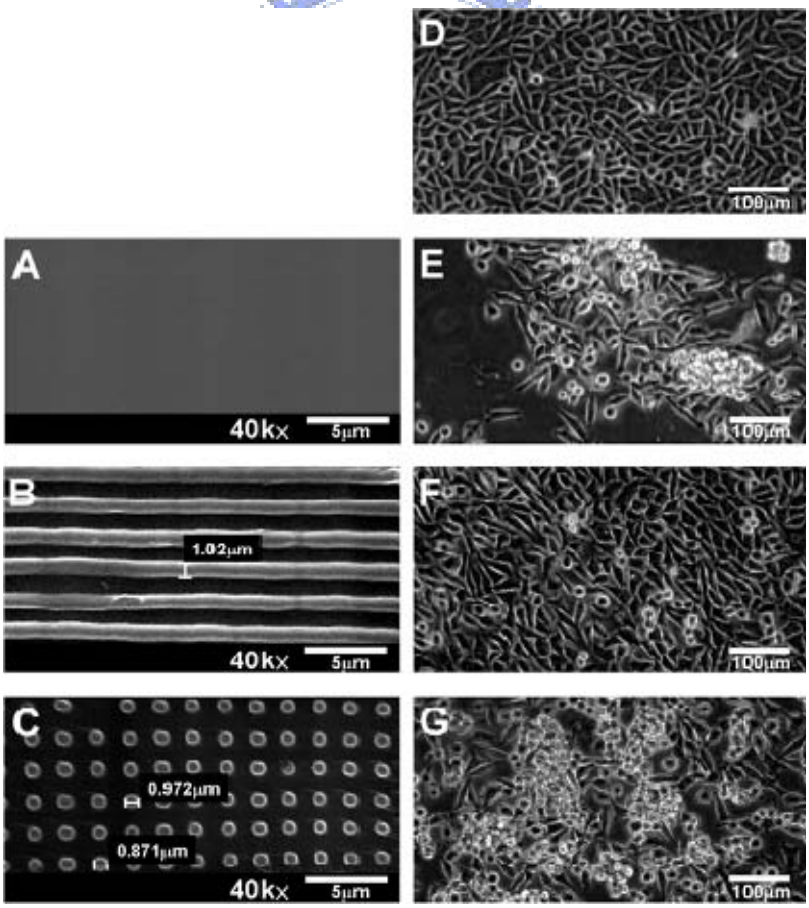

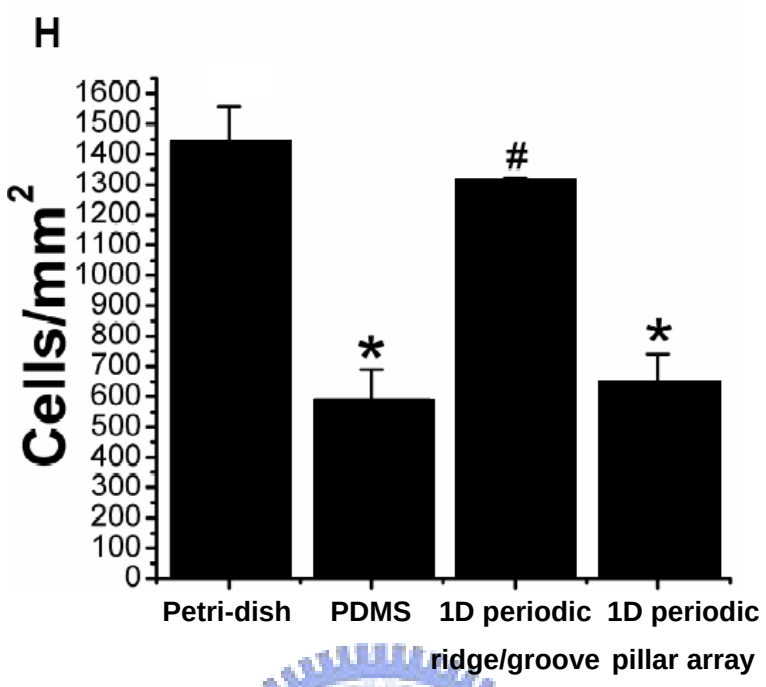

Figure 4.2 SEM images of flat PDMS surface (A), 1D periodic line/space (1μm width) PDMS surface (B) and 2D periodic pillar (1μm diameter) PDMS surface (C). Optical microscope images of HeLa cells cultured for 24h on bacteriological grade polystyrene Petri dish (D), flat PDMS surface (E), 1D periodic line/space patterned PDMS surface (F), and 2D periodic pillar patterned PDMS surface (G). (H) The average number of adherent HeLa cells on different patterned PDMS surface. Statistical significance assessed by one-way ANOVA tests is shown as *:$p < 0.05$ when compared with polystyrene Petri dish control and #: $p < 0.05$ when compared with flat PDMS control.

After the patterned and non-patterned PDMS is carefully removed from silicon mold, the images of features on PDMS surface were collected by scanning electron microscope (shown in **Fig. 4.2A-C**). Feature pitches (sum of the groove and ridge widths) were uniform in each field. And 2D dense lines and dense dots are both on a 2μm pitch with 1μm line width and 1μm dot diameter, both patterns were about 350nm depth. HeLa cervical cancer cells were cultured on patterned and non-patterned PDMS surface for 24hr and direct observed of living cells under an

optical microscope. As shown in Fig. 2D-G, when cells cultured on the 2D periodic pillars and smooth PDMS substrates, cells aggregated and were mostly round and worse adherent. Contrast with cells growth on 1D periodic lines which expressed a normal morphology similar to cells adhere on Petri dish. The growth rate was further quantified. Equal numbers of the cells were seeded at identical conditions and the number of cells at 24 h after seeding was counted at different three positions on each substrates. Relative to those on flat PDMS and 2D periodic pillars with 1μm wide diameter ($p < 0.05$, **Fig. 4.2H**), the average number of adherent HeLa cells (cells/mm^2) after 24hr of culturing was significantly greater on 1D periodic lines with 1μm wide ridges/grooves PDMS surface which revealed no significant differences with Petri dish control.

Furthermore, according to the Ar/O_2-based plasmas treated PDMS surface, untreated PDMS is not a good substrate for supporting cells adhesion and growth well as an extracellular scaffold because of the higher the hydrophobicity, the lesser the cell adhered and cell surface [62]. In agreement on the characteristic of PDMS substrate, we found it was more bio-compatible than untreated smooth PDMS when 1D periodic line patterned on, it is likely that the topography has this positive effect on cell survival (improved adhesion is usually associated with improved survival).

4.2. Cells adhere to flat PDMS and 2D periodic pillars patterned PDMS substrate show a retarded G1/S transition.

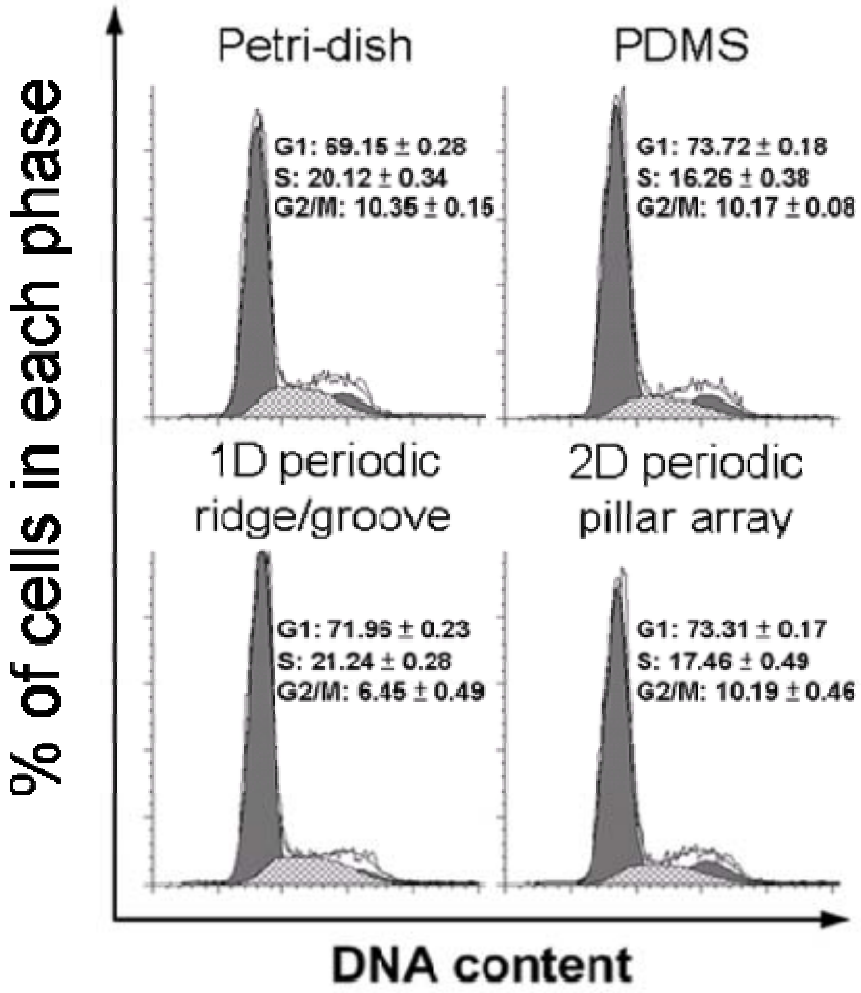

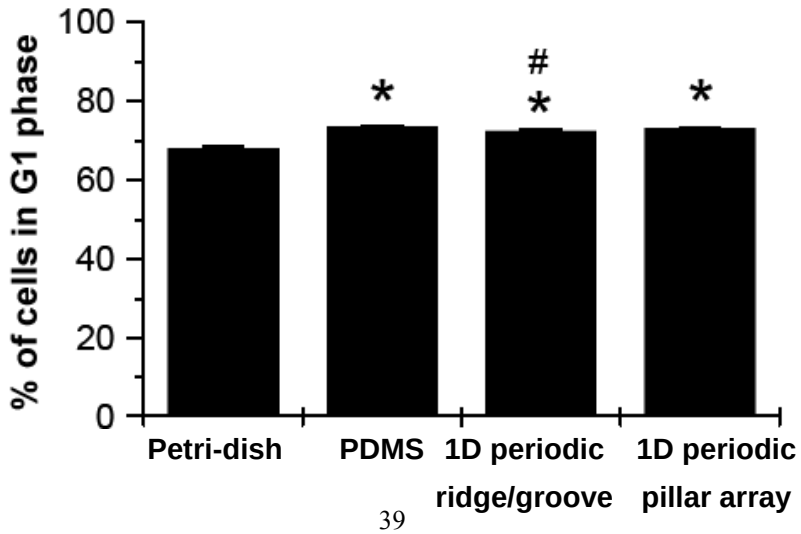

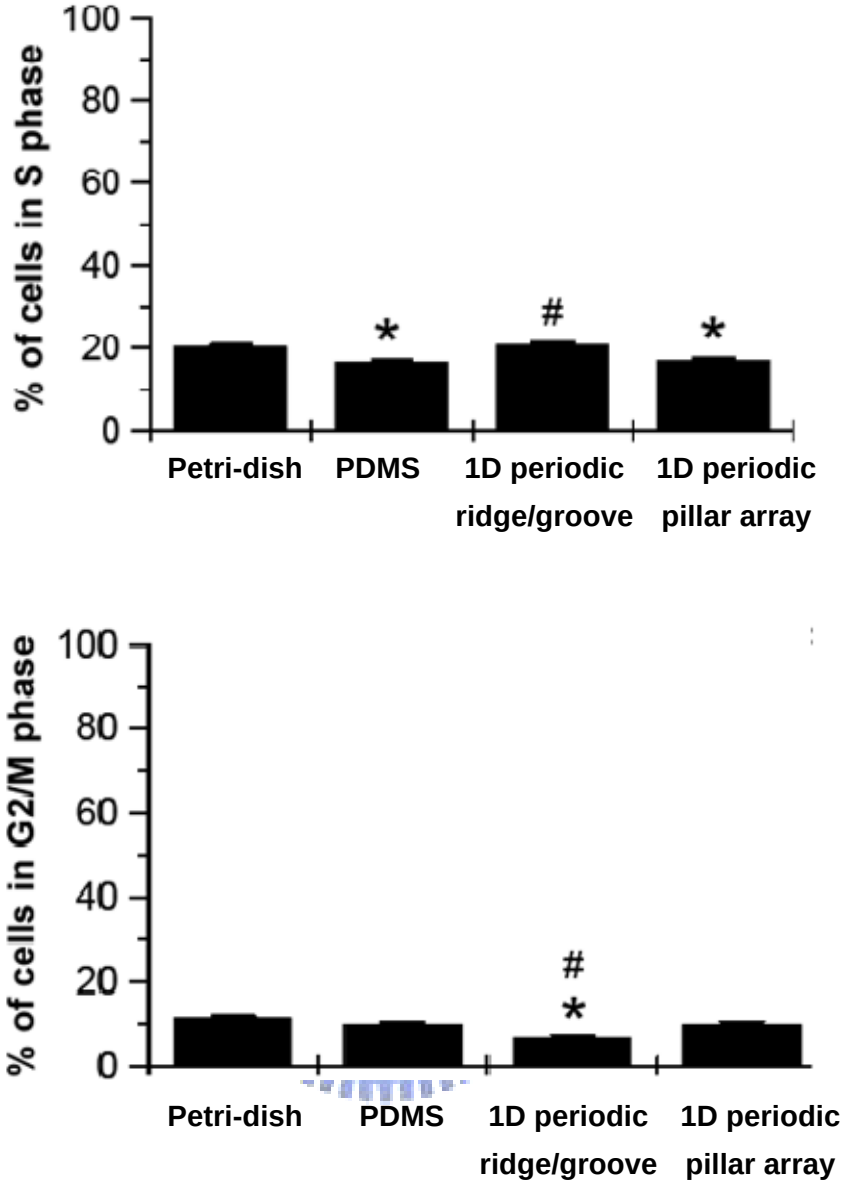

Figure 4.3 Analysis of cell cycle phases. The cell cycle of HeLa cells cultured on smooth and patterned PDMS substrates for 24h. Cellular DNA was stained with propidium iodide and analyzed by flow cytometry. (A) The DNA content of cells of the cell cycle. (B-C) A histogram represents the percentage of total cells in G1 phase, S phase and G2/M phase, respectively. Statistical significance assessed by one-way ANOVA tests is shown as *:$p < 0.05$ when compared with polystyrene Petri dish control and #: $p < 0.05$ when compared with flat PDMS control.

The cell cycle was investigated by comparing the DNA contents of the HeLa cells cultured on Petri dish, smooth and patterned PDMS substrates for 24h and analyzed by flow cytometry **(Fig. 4.3A)**. The DNA content of HeLa cells cultured on Petri dish

showed a cell cycle distribution typical for exponentially growing cells. HeLa cells adhered to flat PDMS and 2D periodic pillars PDMS surface showed a decreased percentage of cells in the S phase and, in contrast an increased percentage of cells in G1 phase **(Fig. 4.3B-C)**. The proportion of tetraploid cells in G2/M phase was much lower when cells adhere on 1D periodic line than on the other surface **(Fig. 4.3D)**. The reduced S phase in the HeLa cells which adhered to flat PDMS and 2D periodic pillars PDMS surface were further verified by measuring the BrdU incorporation. The BrdU incorporation was determined by immunofluorescence and a similar trend was noted for percentage of cells in S phase, as shown by BrdU incorporation. **(Fig. 4.4)**

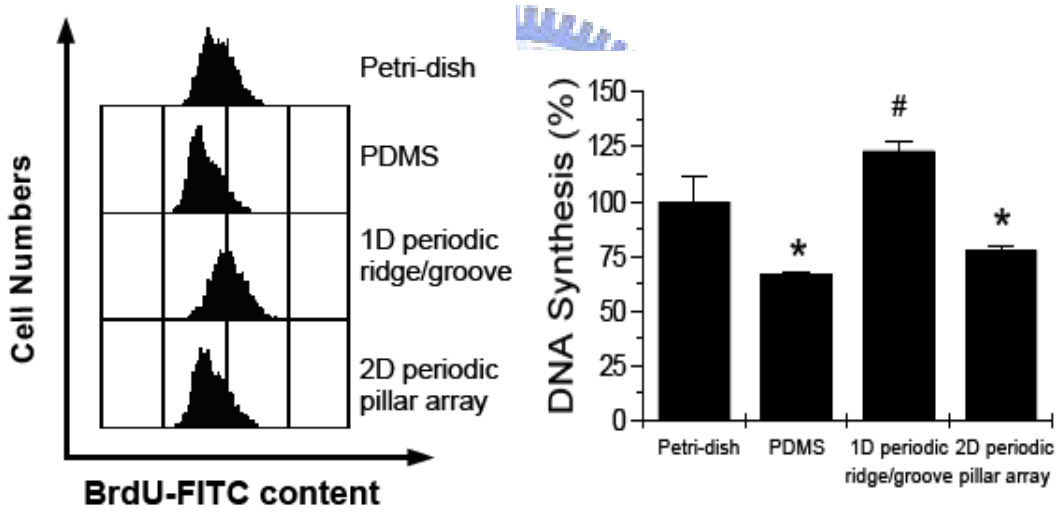

Figure 4.4 BrdU incorporation in HeLa cells cultured on Petri dish, smooth and patterned PDMS substrates. Exponentially growing HeLa cells were incubated with BrdU and the incorporation rate was analysed by immunofluorescence. Statistical analysis was done using ANOVA. The star marks the statistically significant difference in BrdU incorporation at $P < 0.05$ when compared with polystyrene Petri dish control and # marks the statistically significant difference at $p < 0.05$ when compared with flat PDMS control.

Cells adhered on flat PDMS and 2D periodic pillars PDMS substrate showed a significantly decreased incorporation of BrdU. The impaired BrdU incorporation

displayed essentially unchanged on flat PDMS and 2D periodic pillars PDMS surface and was maximal with only 50% BrdU incorporation as compared with those adhered on 1D periodic lines surface. These data confirm the finding of S phase obtained by the analysis of the cellular DNA content, and in agreement with the theory that if a cell cannot flatten fully, it will not enter the S-phase of the cell cycle so readily [63].

4.3. Protein expressed by integrin-mediated intracellular signal transduction.

(A)

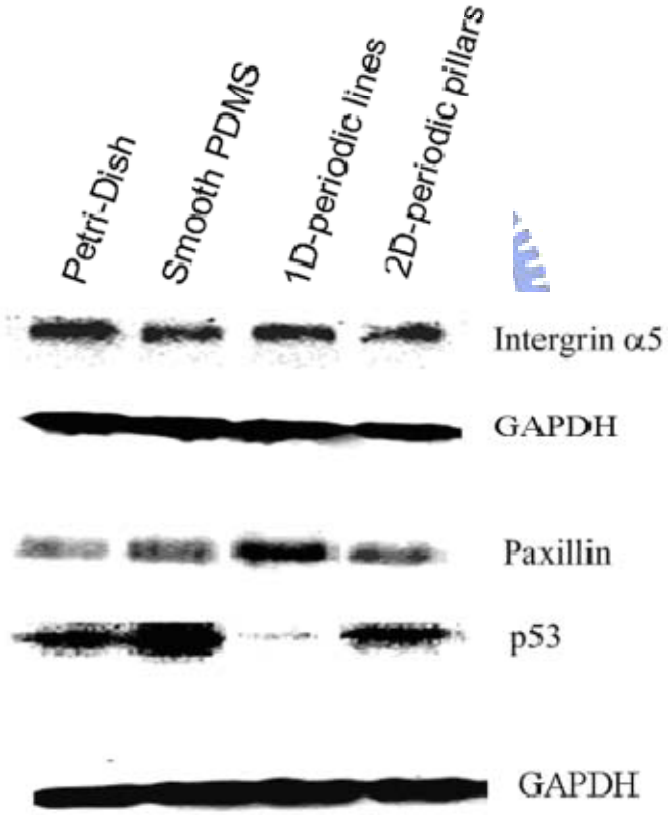

(B)

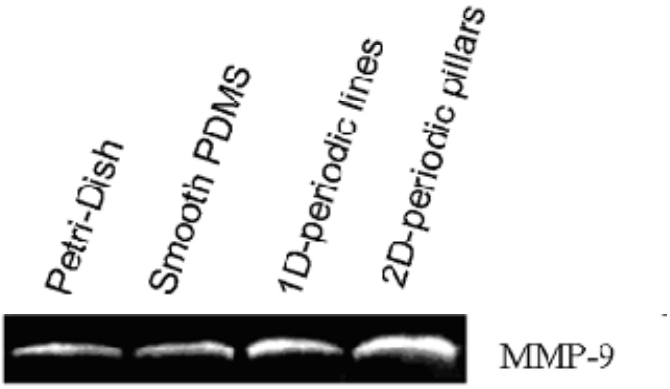

Figure 4.5 (A) Immunoblotting of transmembrane integrin proteins (α5); focal adhesion-associated adaptor protein, paxillin; tumor suppressor protein, p53 (B) Activity of matrix metalloproteinase 9 (MMP-9) analyzed by gelatin zymography.

Different surface topography regulates integrin expression occurs selectively on specific integrin subunits [64]. α5β1 integrin is a cell surface receptor that mediates cell extracellular matrix adhesions by interacting with fibronectin. Studies have shown that FN-α5β1 interaction regulates a variety of cellular responses including gene induction [65], oncogenic transformation [66], differentiation [67], proliferation and cell survival [68] and adhesion and migration [66,69]. Numbers of cranial neural crest cells are undergoing apoptosis along their migration pathways in α5 subunit-deficient embryos could be due to failure of these neural crest cells to migrate to their correct destinations. Nevertheless, they found that α5 is not essential for the survival or normal proliferation of mesodermal cells[70]. In contrast with in vitro studies of Zhang et al. [68] α5 protects against cell death in cultured chinese hamster ovary (CHO) cells, perhaps the difference in the cell growth behavior might be caused by the type of cells involved or differences in cellular environment presented. Up till now it is not clear how topography affects integrin expression.

In our study, western blotting revealed that α5 integrin displayed the variations with respect to micro-scale patterns during the 24hr culture period **(Fig. 4.5 A)**. Level of integrin α5 expression was higher in HeLa cells cultured on 1D periodic lines close to

the cells on Petri dish. The variation of integrin α5 is generally consistent with the tendency of cell attachment **(Fig. 4.2H)** suggesting that micro-topographic PDMS surfaces effect on cells may be mediated by integrin α5 expression.

Paxillin is a cytoskeleton protein involved in actin-membrane attachment at sites of cell adhesion to the extracellular matrix (focal adhesion) [71]. The predicted structure of paxillin suggests that it is a unique cytoskeleton protein capable of interaction with a variety of intracellular signaling and structural molecules important in growth control and the regulation of cytoskeleton organization [72]. According to these reports, our results also found that when cells adhered to 1D periodic lines they spread well accompanying with integrin α5 and paxillin expresse. That is to say, reducing integrin clustering may have resulted in reduced transduction of cell signals to the nucleus, and therefore low rates of proliferation and tissue formation (as shown in **Fig. 4.5A** and bromodeoxyuridine incorporation above-mentioned).

It has been reported when fibroblast contacts a material surface, it must adhere first of all, otherwise it will undergo apoptosis via anoikis (which means homelessness in Greek) [73]. Furthermore, in 1998s, Almeida et al. first report that p53 monitors survival signals from ECM/FAK in anchorage-dependent cells, if FAK or the correct ECM is absent, cells enter apoptosis through a p53-dependent pathway. And this pathway is suppressible by dominant-negative p53. In other words, upon inactivation of p53, cells survive even if they lack matrix signals or FAK [74]. For this reason, it's important to understand how signals from ECM suppress cell death, and what apoptotic pathway is triggered in cells when these signals are lost. In order to investigate the correlation between the signals from external topography and the transduction via transmembrane protein integrin α5 and the anoikis when cells are detached from the ECM, we analyzed the p53 expression on HeLa cells after 24hr culturing on different patterned PDMS surface. Interestingly, there was significantly

reduced p53 as cells cultured on 1D periodic line. In agreement with the theory of p53 controls both the G1 and the G2/M checkpoints and mediates growth arrest [75], cells represented a retarded G1/S transition significantly as HeLa cells adhering to 2D periodic pillars and flat PDMS surface compared with polystyrene Petri dish control ($p < 0.05$, Fig. 3). Oppositely, cells adhered on 1D periodic line with much lower p53 promoted cells to progress into S phase.

Previous reports have shown that MMP-9 was expressed and contributed to early-stage B-cell chronic lymphocytic leukemia (B-CLL) migration through artificial basement membranes or endothelial cells, moreover also contributes to B-CLL progression by facilitating malignant cell migration and tissue invasion [76]. Thus, MMP-9 plays a key role in cell invasion and transendothelial migration and the physiologically up-regulated by integrin also be demonstrated in B-CLL [77].

In this study, we investigated the relation between cell adhesion and expression of active MMP-9 in human epithelial carcinoma HeLa cell line, and also found that accompany with increased α5 integrin protein there were highly expressed MMP-9 when HeLa cells adhered to 2D periodic pillars surface **(Fig. 4.5B)**.. Furthermore, p53 is a negative regulator of MMP-9 gene expression [78], it indicated that MMPs are implicated in tumor cell resistance to the synergistic proapoptotic effect of p53. This is similar to our finding above-mentioned that when HeLa cells were cultured on 1D periodic lines and Petri dish surface, they grow well with suppressed p53 expression. On the contrary, as the HeLa cells adhered on 2D periodic pillars, they showed poor adhesion and spreading properties and accompanied with MMP-9 expression to protect against the proapoptotic effect of p53. For these reasons, we suggest when cells adhere to the proper position of ECM through receptor-integrin interaction, cell progressed and if cells adhere to a worse environment, invasion can be initiated.

4.4. Investigation of cell morphology using scanning electron microscopy.

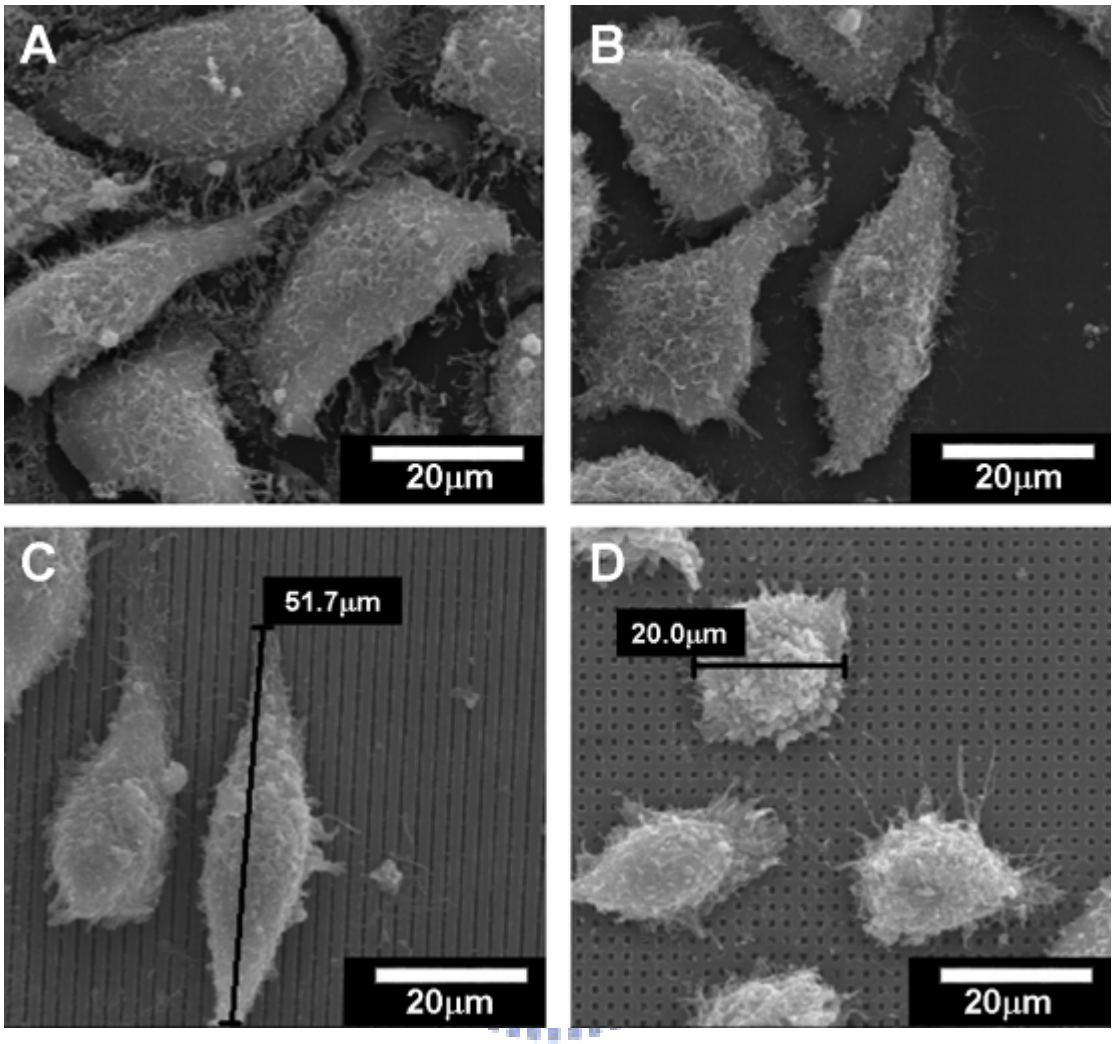

Figure 4.6 Morphology of human epithelial carcinoma HeLa cells cultured on Petri dish (A), smooth bare silicon (native oxide) surface (B), 1D periodic line silicon (native oxide) surface, and 2D periodic pillar silicon (native oxide) surface for 24hr imaged by scanning electron microscopy. Areas of lower cell density were selected to facilitate observation of individual cell shapes. The images of the cells shown in the selected micrographs are typical of cells throughout the culture.

The cells exhibited different shapes on Petri dish, patterned and non-patterned silicon surfaces with native oxide **(Fig. 4.6)**. By way of parenthesis, in the preparation procedures of SEM samples with cells adhered on the surface, it was hard to dehydrate the samples without harming the PDMS substrate (the organic PDMS go through carbonization process and become carbon dust) so here we used silicon oxide

as substrate for observing the cell morphology on patterned and non-patterned surface. Scanning electron micrographs of the cells on the 2D periodic pillar substrates showed that after 24hr seeding, HeLa cells attached with a spherical morphology around 20 μm diameter **(Fig. 4.6D)**. Besides, comparing with the morphology and orientation of cells cultured on smooth substrates and on 2D periodic pillar, cells elongate and align on 1 μm grooves/ridges of 1D periodic line **(Fig. 4.6C)**. The results similar with the cells which adhered on patterned PDMS surface.

In agreement with aligned nanofibers were sufficient to induce neurite elongation and outgrowth and greatly promoted cell migration [79], our results also found that when the external topography induce cells elongation, it is helpful for cell adhesion and proliferation. Moreover the bovine aortic endothelial cells on the nanotube surface facilitate a polarized distribution of contact with a lamellipodial protrusion in the front and the detachment of the tail in the back for accelerated cellular locomotion [80], it is clear that becoming more elongated and mobile form promote cells crawling toward each other and regulate cell to cell communication. On the contrary, similarly to the report of Dalby et al. [81], cells were inhibited from becoming fully flattened to the islands and even expressed a cell cycle arrest, but took on normal morphologies and were able to proliferate and become confluent on the flat controls.

Future research with these topographies should concentrate on casting them into approved polymers and degradable polymers and integrating with normal cell types to improve their usefulness as tissue-engineering scaffolds. Having the ability to control cell adhesion to a material may help in orthopedic and wound-healing procedures, where increased cell adhesion is required, and in applications such as heart valves and catheters, where reduced adhesion is required.

Chapter 5: Conclusions

With the use of an inexpensive and quick method to produce nanotopography, this study has shown a significant cell response in spreading, morphology, cytoskeleton, and proliferation of fibroblasts on the test surfaces. In these results, we found that cell elongation and alignment on grooves and ridges on 1D periodic line/space patterned surface. By contrast, when the cells cultured on the substrate of 2D periodic pillar pattern, they showed poor adhesion and spreading properties accompanying retardation of growth and proliferation. In order to clarify the effects of micro-patterned substrates on DNA content, we chose the substrate with the size of 1 μm periodic line/space pattern and 1 μm periodic pillar pattern for cell cycle analysis. A slight increase of G1 phase population was observed when cells grew on 2D periodic pillar patterned substrate. And a decreased percentage of S phase as cells adhered to flat PDMS and 2D periodic pillars PDMS surface. The reduced S phase with cells which adhered to flat PDMS and 2D periodic pillars PDMS surface were further confirmed by measuring the BrdU incorporation. In contrast, accompanying with S phase increased, a significant decreased of G2/M phase population was observed when cells grew on substrate patterned with 1D periodic line. Moreover, as the focal adhesion proteins decreased, there was an increased expression of tumor suppressor p53, and especially with active MMP-9 released. In conclusion, substrate with 1D periodic line/space pattern promotes cells to appear significant response to elongation and alignment, while substrate with 2D periodic pillar pattern reduces cell adhesion, spreading, growth, proliferation and even promotes metastasis.

Reference

1. Whitesides GM, Ostuni E, Takayama S, Jiang X, Ingber DE. Soft Lithography in biology and biochemistry. Annu Rev Biomed Eng 2001;3:335-373.

2. Chabinyc ML, Chiu DT, McDonald JC, Stroock AD, Christian JF, Karger AM, Whitesides GM. An Integrated Fluorescence Detection System in Poly(dimethylsiloxane) for Microfluidic Applications. Anal Chem 2001;73:4491-4498.

3. Vallet-Regí M. Ceramics for medical applications. J Chem Soc, Dalton Trans 2001;2:97-108.

4. Binyamin G, Shafi BM, Mery CM. Biomaterials: a primer for surgeons. Semin Pediatr Surg 2006;15:276-283.

5. Lutolf MP, Hubbell JA. Synthetic biomaterials as instructive extracellular microenvironments for morphogenesis in tissue engineering. Nat Biotechnol 2005;23:47-55.

6. Langer R, Vacanti JP. Tissue engineering. Science 1993;260:920-926.

7. Khademhosseini A, Langer R, Borenstein J, Vacanti JP. Microscale technologies for tissue engineering and biology. P Natl Acad Sci USA 2006;103:2480-2487.

8. Atala A. Tissue engineering, stem cells and cloning: current concepts and changing trends. Expert Opin Biol Ther 2005;5:879-892.

9. Bianco P, Robey PG. Stem cells in tissue engineering. Nature 2001;414:118-121.

10. Ruszczak Z, Schwartz RA. Modern aspects of wound healing: an update. Dermatol Surg 2000;26:219-229.

11. Wilson CJ, Clegg RE, Leavesley DI, Pearcy MJ. Mediation of biomaterial-cell interactions by adsorbed proteins: a review. Tissue Eng 2005;11:1-18.

12. Kasemo B, Lausmaa J. Surface science aspects on inorganic biomaterials. CRC Crit Rev Biocomp 1986;2:335-380.

13. Park H, Cannizzaro C, Vunjak-Novakovic G, Langer R, Vacanti CA, Farokhzad OC. Nanofabrication and microfabrication of functional materials for tissue engineering. Tissue Eng 2007;13:1867-1877.

14. Kasemo B. Biological surface science. Surf Sci 2002;500:656-677.

15. Andersson H, Berg A. Microfabrication and microfluidics for tissue engineering: state of the art and future opportunities. Lab Chip 2004;4:98-103.

16. Flemming RG, Murphy CJ, Abrams GA, Goodman SL, Nealey PF. Effects of synthetic micro-and nano-structured surfaces on cell behavior. Biomaterials 1999;20:573-588.

17. Braber ET, Ruijter JE, Ginsel LA, Smits HTJ, Recum AF, Jansen JA. Effect of parallel surface microgrooves and surface energy on cell growth. J Biomed Mater Res 1995;29:511-518.

18. Wójciak-Stothard B, Madeja Z, Korohoda W, Curtis A, Wilkinson C. Activation of macrophage-like cells by multiple grooved substrata. Topographical control of cell behaviour. Cell Biol Int 1995;19:485-490.

19. Oakley C, Brunette DM. Response of single, pairs, and clusters of epithelial cells to substratum topography. Biochem Cell Biol 1995;73:473-490.

20. Ohara PT, Buck RC. Contact guidance in vitro. A light, transmission, and scanning electron microscopic study. Exp Cell Res 1979;121:235-249.

21. Meyle J, Gültig K, Brich M, Hämmerle H, Nisch W. Contact guidance of fibroblasts on biomaterial surfaces. J Mater Sci Mater Med 1994;5:463-466.

22. Rosdy M, Grisoni B, Clauss LC. Proliferation of normal human keratinocytes on silicone substrates. Biomaterials 1991;12:511-517.

23. Campbell CE, von Recum AF. Microtopography and soft tissue response. J Invest Surg 1989;2:51-74.

24. Fujimoto K, Takahashi T, Miyaki M, Kawaguchi H. Cell activation by the micropatterned surface with settling particles. J Biomater Sci Polym Ed 1997;8:879-891.

25. Rovensky YA. Morphogenetic response of cultured normal and transformed fibroblasts, and epitheliocytes, to a cylindrical substratum surface. Possible role for the actin filament bundle pattern. J Cell Sci 1994;107:1255-1263.

26. Martin JY, Schwartz Z, Hummert TW, Schraub DM, Simpson J, Lankford Jr. J, Dean DD, Cochran DL, Boyan BD. Effect of titanium surface roughness on proliferation, differentiation, and protein synthesis of human osteoblast-like cells (MG63). J Biomed Mater Res 1995;29:389-401.

27. Eisenbarth E, Meyle J, Nachtigall W, Breme J. Influence of the surface structure of titanium materials on the adhesion of fibroblasts. Biomaterials 1996;17:1399-1403.

28. Rich A. Anomalous preferences of cultured macrophages for hydrophobic and roughened substrata. J Cell Sci 1981;50:1-7.

29. Wilkinson PC, Shields JM, Haston WS. Contact guidance of human neutrophil leukocytes. Exp Cell Res 1982;140:55-62.

30. Goodman SL, Sims PA, Albrecht RM. Three-dimensional extracellular matrix textured biomaterials. Biomaterials 1996;17:2087-2095.

31. Robbie K, Brett MJ. Sculptured thin films and glancing angle deposition: Growth mechanics and applications. J Vac Sci Technol A 1997;15:1460-1465.

32. Phillips HM, Sauerbrey RA. Excimer-laser-produced nanostructures in polymers. Opt Eng 1993;32:2424-2436.

33. McClelland JJ, Scholten RE, Palm EC, Celotta RJ. Laser-focused atomic deposition. Science 1993;262:877-880.

34. Xia Y, Kim E, Zhao XM, Rogers JA, Prentiss M, Whitesides GM. Complex optical surfaces formed by replica molding against elastomeric masters. Science 1996;273:347-349.

35. Chou SY, Krauss PR, Renstrom PJ. Imprint of sub-25 nm vias and trenches in polymers. Appl Phys Lett 1995;67:3114-3116.

36. Giordano RA, Wu BM, Borland SW, Cima LG, Sachs EM, Cima MJ. Mechanical properties of dense polylactic acid structures fabricated by three dimensional printing. J Biomater Sci Polym Ed 1997;8:63-75.

37. Griffith LG, Wu B, Cima MJ, Powers MJ, Chaignaud B, Vacanti JP. In Vitro Organogenesis of Liver Tissue. Ann NY Acad Sci 1997;831:382-397.

38. Weiss P. Cell contact. Int Rev Cytol 1958;7:391-423.

39. Rosenberg MD. Long-range interactions between cell and substratum. P Natl Acad Sci USA 1962;48:1342-1349.

40. Den Braber ET, De Ruijter JE, Ginsel LA, Von Recum AF, Jansen JA. Orientation of ECM protein deposition, fibroblast cytoskeleton, and attachment complex components on silicone microgrooved surfaces. J Biomed Mater Res 1998;40:291-300.

41. Chehroudi B, McDonnell D, Brunette DM. The effects of micromachined surfaces on formation of bonelike tissue on subcutaneous implants as assessed by radiography and computer image processing. J Biomed Mater Res 1997;34:279-290.

42. Mrksich M, Chen CS, Xia Y, Dike LE, Ingber DE, Whitesides GM. Controlling cell attachment on contoured surfaces with self-assembled monolayers of alkanethiolates on gold. P Natl Acad Sci USA 1996;93:10775-10778.

43. Hoch HC, Staples RC, Whitehead B, Comeau J, Wolf ED. Signaling for growth orientation and cell differentiation by surface topography in Uromyces. Science 1997;235:1659-1662.

44. Green AM, Jansen JA, Van der Waerden J, Von Recum AF. Fibroblast response to microtextured silicone surfaces: Texture orientation into or out of the surface. J Biomed Mater Res 1994;28:647-653.

45. Fewster SD, Coombs RRH, Kitson J, Zhou S. Precise ultrafine surface texturing of implant materials to improve cellular adhesion and biocompatibility. Nanobiology 1994;3:201-214.

46. Wojciak-Stothard B, Denyer M, Mishra M, Brown RA. Adhesion, orientation, and movement of cells cultured on ultrathin fibronectin fibers. In Vitro Cell Dev-An 1997;33:110-117.

47. Teixeira AI, Abrams GA, Bertics PJ, Murphy CJ, Nealey PF. Epithelial contact guidance on well-defined micro-and nanostructured substrates. J Cell Sci 2003;116:1881-1892.

48. Oakley C. The sequence of alignment of microtubules, focal contacts and actin filaments in fibroblasts spreading on smooth and grooved titanium substrata. J Cell Sci 1993;106:343-354.

49. Riveline D, Zamir E, Balaban NQ, Schwarz US, Ishizaki T, Narumiya S, Kam Z, Geiger B, Bershadsky AD. Focal contacts as mechanosensors externally applied local mechanical force induces growth of focal contacts by an mDia1-dependent and ROCK-independent mechanism. J Cell Biol 2001;153:1175-1186.

50. Dunn GA. Alignment of fibroblasts on grooved surfaces described by a simple geometric transformation. J Cell Sci 1986;83:313-340.

51. Chen CS, Mrksich M, Huang S, Whitesides GM, Ingber DE. Geometric control of cell life and death. Science 1997;276:1425-1428.

52. Kleinman HK, Philp D, Hoffman MP. Role of the extracellular matrix in morphogenesis. Curr Opin Biotechnol 2003;14:526-532.

53. Emsley J, Knight CG, Farndale RW, Barnes MJ, Liddington RC. Structural basis of collagen recognition by integrin α2β1. Cell 2000;101:47-56.

54. Marquis ME, Lord E, Bergeron E, Drevelle O, Park H, Cabana F, Senta H, Faucheux N. Bone cells-biomaterials interactions. Front Biosci 2009;14:1023-1067.

55. Bijian K, Takano T, Papillon J, Khadir A, Cybulsky AV. Extracellular matrix regulates glomerular epithelial cell survival and proliferation. Am J Physiol Renal Physiol 2004;286:255-266.

56. Ingber DE. Cellular mechanotransduction: putting all the pieces together again. Faseb J 2006;20:811-827.

57. Ilic D, Almeida EAC, Schlaepfer DD, Dazin P, Aizawa S, Damsky CH. Extracellular matrix survival signals transduced by focal adhesion kinase suppress p53-mediated apoptosis. J Cell Biol 1998;143:547-560.

58. Ko LJ, Prives C. p53: puzzle and paradigm. Genes Dev 1996;10:1054-1072.

59. Frisch SM, Ruoslahti E. Integrins and anoikis. Curr Opin Cell Biol 1997;9:701-706.

60. Shackelford JF, Clode MP. Introduction to materials science for engineers. 4th ed. New Jersey: Prentice Hall Inc: Upper Saddle River, 1996.

61. Teixeira AI, Abrams GA, Bertics PJ, Murphy CJ, Nealey PF. Epithelial contact guidance on well-defined micro-and nanostructured substrates. J Cell Sci 2003;116:1881-1892.

62. Fuard D, Tzvetkova-Chevolleau T, Decossas S, Tracqui P, Schiavone P. Optimization of Poly-Di-Methyl-Siloxane (PDMS) substrates for studying cellular adhesion and motility. Microelectron Eng 2008;85:1289-1293.

63. Alberts B, Bray D, Lewis J, Raff M, Roberts K, Watson JD. Molecular biology of the cell. 3rd ed. New York: Garland Publishing, 1994.

64. Lim JY, Dreiss AD, Zhou Z, Hansen JC, Siedlecki CA, Hengstebeck RW, Cheng J, Winograd N, Donahue HJ. The regulation of integrin-mediated osteoblast focal adhesion and focal adhesion kinase expression by nanoscale topography. Biomaterials 2007;28:1787-1797.

65. Huhtala P, Humphries M, McCarthy J, Tremble P, Werb Z, Damsky C. Cooperative signaling by alpha 5 beta 1 and alpha 4 beta 1 integrins regulates metalloproteinase gene expression in fibroblasts adhering to fibronectin. J Cell Biol 1995;129:867-879.

66. Giancotti FG, Ruoslahtl E. Elevated levels of the α5β1 fibronectin receptor suppress the transformed phenotype of Chinese hamster ovary cells. Cell 1990;60:849-859.

67. Adams JC, Watt FM. Changes in keratinocyte adhesion during terminal differentiation: Reduction in fibronectin binding precedes α5β1 integrin loss from the cell surface. Cell 1990;63:425-435.

68. Zhang Z, Vuori K, Reed JC, Ruoslahti E. The alpha 5 beta 1 integrin supports survival of cells on fibronectin and up-regulates Bcl-2 expression. P Natl Acad Sci USA 1995;92:6161-6165.

69. Akiyama S, Yamada S, Chen W, Yamada K. Analysis of fibronectin receptor function with monoclonal antibodies: roles in cell adhesion, migration, matrix assembly, and cytoskeletal organization. J Cell Biol 1989;109:863-875.

70. Goh KL, Yang JT, Hynes RO. Mesodermal defects and cranial neural crest apoptosis in alpha5 integrin-null embryos. Development 1997;124:4309-4319.

71. Salgia R, Li JL, Lo SH, Brunkhorst B, Kansas GS, Sobhany ES, Sun Y, Pisick E, Hallek M, Ernst T. Molecular Cloning Of Human Paxillin, a Focal Adhesion Protein Phosphorylated by P210. J Biol Chem 1995;270:5039-5047.

72. Turner CE, Miller JT. Primary sequence of paxillin contains putative SH_2 and SH_3 domain binding motifs and multiple LIM domains: identification of a vinculin and pp125Fak-binding region. J Cell Sci 1994;107:1583-1591.

73. Frisch S, Francis H. Disruption of epithelial cell-matrix interactions induces apoptosis. J Cell Biol 1994;124:619-626.

74. Almeida EAC, Schlaepfer DD, Dazin P, Aizawa S, Damsky CH. Extracellular Matrix Survival Signals Transduced by Focal Adhesion Kinase Suppress p53-mediated Apoptosis. J Cell Biol 1998;143:547-560.

75. Agarwal ML, Agarwal A, Taylor WR, Stark GR. p53 controls both the G2/M and the G1 cell cycle checkpoints and mediates reversible growth arrest in human fibroblasts. P Natl Acad Sci USA 1995;92:8493-8497.

76. Kamiguti AS, Lee ES, Till KJ, Harris RJ, Glenn MA, Lin K, Chen HJ, Zuzel M, Cawley JC. The role of matrix metalloproteinase 9 in the pathogenesis of chronic lymphocytic leukaemia. Brit J Haem 2004;125:128-140.

77. Redondo-Munoz J, Escobar-Diaz E, Samaniego R, Terol MJ, Garcia-Marco JA, Garcia-Pardo A. MMP-9 in B-cell chronic lymphocytic leukemia is up-regulated by {alpha}4beta1 integrin or CXCR4 engagement via distinct signaling pathways, localizes to podosomes, and is involved in cell invasion and migration. Blood 2006;108:3143-3151.

78. Meyer E, Vollmer J, Bovey R, Stamenkovic I. Matrix Metalloproteinases 9 and 10 Inhibit Protein Kinase C-Potentiated, p53-Mediated Apoptosis. Cancer Res 2005;65:4261-4272.

79. Patel S, Kurpinski K, Quigley R, Gao H, Hsiao BS, Poo M, Li S. Bioactive Nanofibers: Synergistic Effects of Nanotopography and Chemical Signaling on Cell Guidance. Nano Lett 2007;7:2122-2128.

80. Brammer KS, Oh S, Gallagher JO, Jin S. Enhanced Cellular Mobility Guided by TiO_2 Nanotube Surfaces. Nano Lett 2008;8:786-793.

81. Dalby MJ, Childs S, Riehle MO, Johnstone HJH, Affrossman S, Curtis ASG. Fibroblast reaction to island topography: changes in cytoskeleton and morphology with time. Biomaterials 2003;24:927-935.